Mode-coupling theory for the slow collective dynamics of fluids adsorbed in disordered porous media

V. Krakoviack

Laboratoire de Chimie, UMR CNRS 5182, École Normale Supérieure de Lyon, 46 Allée d'Italie, 69364 Lyon cedex 07, France

We derive a mode-coupling theory for the slow dynamics of fluids confined in disordered porous media represented by spherical particles randomly placed in space. Its equations display the usual nonlinear structure met in this theoretical framework, except for a linear contribution to the memory kernel which adds to the usual quadratic term. The coupling coefficients involve structural quantities which are specific of fluids evolving in random environments and have expressions which are consistent with those found in related problems. Numerical solutions for two simple models with pure hard core interactions lead to the prediction of a variety of glass transition scenarios, which are either continuous or discontinuous and include the possibility of higher-order singularities and glass-glass transitions. The main features of the dynamics in the two most generic cases are reviewed and illustrated with detailed computations. Moreover, a reentry phenomenon is predicted in the low fluid-high matrix density regime and is interpreted as the signature of a decorrelation mechanism by fluid-fluid collisions competing with the localization effect of the solid matrix.

I. INTRODUCTION

Over the past fifteen years, the dynamics of glass-forming liquids under nanoscale confinement has attracted much attention. A great variety of molecular systems under many different types of confinement has been subjected to virtually all available experimental techniques, while at the same time extensive studies of simple model systems using molecular dynamics simulations were undertaken [1–4].

The main reason for this rapidly growing interest is that confinement is considered as a potential tool to investigate the concept of cooperativity, a key ingredient of many glass transition theories [5–7]. Indeed, there are now many evidences that the dynamics of deeply supercooled liquids is inhomogeneous and that dynamically correlated groups of molecules play a crucial role in the slowing down of the dynamics when the temperature is decreased. But, up to now, many questions pertaining, for instance, to the shape, size, or temperature evolution of these dynamical heterogeneities remain essentially unanswered (for recent progress, see, however, Ref. [8]).

In confinement, geometric constraints associated with the pore shape are imposed to the adsorbed fluid and new characteristic length scales, like the pore size, come into play. Thus, by looking for alterations in the dynamics under confinement compared to the bulk, one can hope to pinpoint some of the elusive characteristic features of the dynamical heterogeneities. For instance, in the simplest scenarios, deviations from the bulk behavior are expected to occur due to finite size effects, when the typical size of the dynamical heterogeneities in the bulk would become larger than the pore size. Confinement effects would thus provide a ruler to measure dynamical heterogeneities.

The situation actually turns out more complex. Indeed, a direct comparison between the bulk and confined fluids is only meaningful if the physical phenomena which are specific to confinement have a weak impact on the properties of the imbibed fluid or at least if their influence is sufficiently well understood that it can be corrected for. This is usually not so and strong confinement effects are often observed, for instance, the formation of structured layers of almost immobile molecules at the fluid-solid interface. So, in fact, dynamics in confinement should be addressed as a problem of its own, not necessarily with reference to the bulk.

The variety of the systems to consider is immense. Porous media can differ in the size, shape, and topology of their pore space. They can be made of various materials or receive different surface treatments, leading to a wide range of fluid-solid interactions which adds to the already great variability of the intermolecular interactions met with usual glass formers. Thus, owing to the complexity of the field, a reasonable microscopic theory, able to catch at least some of these aspects, could be very helpful. Indeed, applied to various models, it would allow us to explore thoroughly the phenomenology of confined glass-forming liquids and maybe to disentangle the contributions of the different physical phenomena which interplay in these systems.

Many porous media, like controlled porous glasses and aerogels, are disordered. In the past few years, a very useful and quite successful model to deal with this kind of system has been the so-called "quenched-annealed" (QA) binary mixture, first introduced by Madden and Glandt [9,10]. In this model, sketched in Fig. 1, the fluid molecules (the annealed component) equilibrate in a matrix of particles frozen in a disordered configuration sampled from a given probability distribution (the quenched component). The matrix is assumed to be statistically homogeneous, so that, while for any single realization, the system lacks translational and rotational invariance, all expectation values computed with the matrix probability distribution will have the same properties as in a truly translationally and rotationally invariant system. A common, but not unique, prescription is to take the equilibrium distribution of some simple fluid system, so that the various samples of the matrix can be thought of as the results of instantaneous thermal quenches of this original equilibrium system, hence the denomination "quenched" for the matrix component.
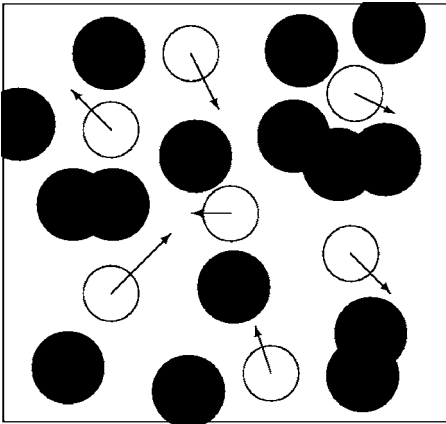
FIG. 1. Sketch of a QA system. In black, the immobile matrix particles. In white, with arrows symbolizing their movement, the fluid particles.

11Thanks to the assumption of statistical homogeneity, as far as the computation of matrix averaged quantities is concerned, QA mixtures can be studied with great ease using simple extensions of standard liquid state theoretical methods. This has been put to good use to derive equations describing the structure and the thermodynamics of these systems, either via diagrammatic techniques [9–11] or by application of the replica trick [12–15].

The aim of the present work is now to develop a dynamical theory for QA mixtures able to deal with the problem of the glass transition in confinement. This will take the form of an extension to QA systems of the ideal mode-coupling theory (MCT) for the liquid-glass transition [16–20]. The MCT occupies a central place in the study of the dynamics of supercooled liquids in the bulk, as one of the very few available microscopic theories in this field. It has well known deficiencies, in particular the fact that its predicted sharp ergodicity breaking transition, the so-called ideal glass transition, is always located in the regime of weak to mild supercooling, rather far from the calorimetric glass transition point. But, quite remarkably, it has been able to correctly predict novel nontrivial relaxation patterns which develop in systems like colloidal suspensions with short-ranged attractions [21] or fluids of symmetric dumbbells [22], when the parameters of these models are varied. It seems thus sensible to turn to this theoretical framework for a systematic investigation of confined glass-forming liquids, aiming at understanding, at least qualitatively, how the microscopic details of the fluid-solid system impact its dynamics. Moreover, it is encouraging that recent computer simulation data for confined fluids could be interpreted with the universal predictions of the MCT [23–25], showing that the mode-coupling glass transition scenario might indeed be of some relevance in confinement as well. Note that Ref. [24] precisely deals with a QA system, as do Refs. [26–28], where other simulation studies are reported.

Theories related to the one to be derived have already been discussed in the literature. The mode-coupling approach to the diffusion-localization transition in the classical random Lorentz gas [29–31] is of particular relevance, since this system is actually a QA mixture taken in the limit of a vanishing density of the annealed component. Besides, the present theory will borrow some ideas from this approach. Other works have dealt with the conductor-insulator transition of quantum fluids in random potentials, originally neglecting the fluid-fluid interactions [32,33] which were later reintroduced by Thakur and Neilson [34]. They appear as special cases of the present theory, with additional implicit and uncontrolled approximations in the treatment of the effect of randomness on the static fluid correlations [35]. Finally, a similar nonlinear feedback mechanism has been derived for the freezing of a polymer chain in a quenched random medium using the self-consistent Hartree approximation for the Langevin dynamics of the system [36].

The paper is organized as follows. In Sec. II, the MCT equations for the collective dynamics of a QA mixture are derived and discussed, while Sec. III explores the relation between the dynamics in a self-induced glassy phase and in a quenched random environment. In Sec. IV, dynamical phase diagrams for two simple models are computed, which show two basic types of ideal liquid-glass transitions discussed in more details in Sec. V. Section VI is devoted to concluding remarks. Preliminary reports on the present work can be found in Refs. [37]. and [38]

II. MODE-COUPLING THEORY FOR QUENCHED-ANNEALED SYSTEMS

In this section, the mode-coupling equations for the QA binary mixture are derived and discussed. But, before proceeding with the dynamical theory, a few static quantities have to be defined.

As mentioned in the Introduction, in a QA system, the disordered porous medium is represented by a collection of N_m rigorously immobile point particles, randomly placed in a volume V at positions denoted by $\mathbf{s}_1, \mathbf{s}_2, \ldots, \mathbf{s}_{N_m}$, according to a given probability distribution $\mathcal{P}(\mathbf{s}_1, \mathbf{s}_2, \ldots, \mathbf{s}_{N_m})$ [9,10]. Its overall density is $n_m = N_m/V$ and the Fourier components of its frozen microscopic density, or, in short, its frozen density fluctuations, are given by

$$\rho_{\mathbf{q}}^m = \sum_{j=1}^{N_m} e^{i\mathbf{q}\cdot\mathbf{s}_j}, \tag{1}$$

where $\mathbf{q}$ denotes the wave vector. Their disorder-averaged correlation functions, which, because of the assumed statistical homogeneity, are diagonal in $\mathbf{q}$ and only depend on its modulus q, define the matrix structure factor

$$S_q^{mm} = \frac{1}{N_m} \overline{\rho_{\mathbf{q}}^m \rho_{-\mathbf{q}}^m}, \tag{2}$$

where $\overline{\cdots}$ denotes an average over the matrix realizations.

The fluid component consists of N_f point particles (density $n_f = N_f/V$) of mass m, which equilibrate at a temperature T in the random potential energy landscape created by the frozen matrix particles. As in the bulk, for the present theory, we will be interested in the dynamics of the fluid density fluctuations

$$\rho_{\mathbf{q}}^f(t) = \sum_{j=1}^{N_f} e^{i\mathbf{q}\cdot\mathbf{r}_j(t)}, \tag{3}$$

where $\mathbf{r}_j(t)$ is the position of the fluid particle j at time t. At equal times, they allow us to define the fluid structure factor

$$S_q^{ff} = \frac{1}{N_f}\overline{\langle \rho_{\mathbf{q}}^f \rho_{-\mathbf{q}}^f \rangle}, \tag{4}$$

and the fluid-matrix structure factor

$$S_q^{fm} = \frac{1}{\sqrt{N_f N_m}}\overline{\langle \rho_{\mathbf{q}}^f \rho_{-\mathbf{q}}^m \rangle}, \tag{5}$$

where $\langle \cdots \rangle$ denotes a thermal average *taken for a given realization of the matrix*, the disorder average $\overline{\cdots}$ being performed *subsequently*.

For an ordinary binary mixture, the knowledge of the above three structure factors would be enough to fully characterize the structure at the pair level. This is not the case for a QA mixture. Indeed, because the matrix component is quenched, for any single realization, the system lacks translational and rotational invariance. It results that, at variance with a bulk fluid, nonzero average density fluctuations exist at equilibrium, i.e., $\langle \rho_{\mathbf{q}}^f \rangle \neq 0$. It is only after averaging over disorder that the symmetry is restored, so that $\overline{\langle \rho_{\mathbf{q}}^f \rangle} = 0$. Thus one is led to consider relaxing and nonrelaxing fluid density fluctuations, corresponding to $\delta\rho_{\mathbf{q}}^f(t) = \rho_{\mathbf{q}}^f(t) - \langle \rho_{\mathbf{q}}^f \rangle$ and $\langle \rho_{\mathbf{q}}^f \rangle$, respectively, and to define the connected fluid structure factor

$$S_q^c = \frac{1}{N_f}\overline{\langle \delta\rho_{\mathbf{q}}^f \delta\rho_{-\mathbf{q}}^f \rangle}, \tag{6}$$

and the disconnected or blocked fluid structure factor

$$S_q^b = \frac{1}{N_f}\overline{\langle \rho_{\mathbf{q}}^f \rangle \langle \rho_{-\mathbf{q}}^f \rangle}, \tag{7}$$

such that $S_q^{ff} = S_q^c + S_q^b$. This splitting of the fluid pair correlations is well known from the replica theory of QA systems, where it leads to the peculiar structure of the so-called replica Ornstein-Zernike (OZ) equations [12–15], which are given in Appendix A for reference.

Nonzero average fluid density fluctuations at equilibrium mean that, even without any dynamical ergodicity breaking, they will have time-persistent correlations. Indeed, defining the normalized total density fluctuation autocorrelation function

$$\phi_q^T(t) = \frac{\overline{\langle \rho_{\mathbf{q}}^f(t) \rho_{-\mathbf{q}}^f(0) \rangle}}{N_f S_q^{ff}}, \tag{8}$$

one expects using standard arguments that

$$\lim_{t\to\infty} \phi_q^T(t) = \frac{\overline{\langle \rho_{\mathbf{q}}^f \rangle \langle \rho_{-\mathbf{q}}^f \rangle}}{N_f S_q^{ff}} = \frac{S_q^b}{S_q^{ff}} > 0. \tag{9}$$

This is a general consequence of the fact that the fluid evolves in an inhomogeneous environment and we stress that this is a true static phenomenon.

Usually, mode-coupling theories are derived assuming that the statics of the problem is solved. For this reason, since the calculation of the contribution from the blocked correlations is actually a static problem, the theory has been developed using the relaxing part of the fluid density fluctuations as the central dynamical variable. Attempts to derive a dynamical theory starting from the full density fluctuations have resulted in complicated equations, which appeared unfaithful to the statics of the problem, and thus were abandoned.

The theory is derived using standard projection operator methods, as shown in Ref. [18] for bulk systems. As usual, in a first step, one obtains a generalized Langevin equation for the time evolution of the normalized connected autocorrelation function of the density fluctuations

$$\phi_q(t) = \frac{\overline{\langle \delta\rho_{\mathbf{q}}^f(t) \delta\rho_{-\mathbf{q}}^f(0) \rangle}}{N_f S_q^c}. \tag{10}$$

It is formally the same as for the bulk, i.e.,

$$\ddot{\phi}_q(t) + \Omega_q^2 \phi_q(t) + \Omega_q^2 \int_0^t d\tau\, m_q(t-\tau)\dot{\phi}_q(\tau) = 0, \tag{11}$$

with initial conditions $\phi_q(0) = 1$, $\dot{\phi}_q(0) = 0$, and

$$\Omega_q^2 = \frac{q^2 k_B T}{m S_q^c}. \tag{12}$$

The second step involves the calculation of the slow decaying portion of the memory kernel $m_q(t)$ with a mode-coupling approach. We will assume that the slow dynamics is dominated by three types of quadratic variables, which can be separated in two classes. In the first class, we have variables quadratic in the relaxing density fluctuations, $\delta\rho_{\mathbf{k}}^f \delta\rho_{\mathbf{q}-\mathbf{k}}^f$, in close analogy with bulk MCT [16]. In the second class, inspired by previous studies on the Lorentz gas [29–31], we consider variables expressing couplings of the relaxing density fluctuations to the two frozen density fluctuations present in the problem, $\delta\rho_{\mathbf{k}}^f \rho_{\mathbf{q}-\mathbf{k}}^m$ and $\delta\rho_{\mathbf{k}}^f \langle \rho_{\mathbf{q}-\mathbf{k}}^f \rangle$. The last variable was omitted in all previous works, including a recent account of the present theory [37], with consequences to be discussed below.

The calculation is outlined in Appendix B and we only quote the result here. It reads $m_q(t) = \Gamma_q \delta(t) + m_q^{(MC)}(t)$, where Γ_q is a friction coefficient associated with fast dynamical processes, and

$$m_q^{(MC)}(t) = \int \frac{d^3\mathbf{k}}{(2\pi)^3}[V_{\mathbf{q},\mathbf{k}}^{(2)}\phi_k(t)\phi_{|\mathbf{q}-\mathbf{k}|}(t) + V_{\mathbf{q},\mathbf{k}}^{(1)}\phi_k(t)], \tag{13}$$

with

$$V_{\mathbf{q},\mathbf{k}}^{(2)} = \frac{1}{2}n_f S_q^c \left[\frac{\mathbf{q}\cdot\mathbf{k}}{q^2}\hat{c}_k^c + \frac{\mathbf{q}\cdot(\mathbf{q}-\mathbf{k})}{q^2}\hat{c}_{|\mathbf{q}-\mathbf{k}|}^c \right]^2 S_k^c S_{|\mathbf{q}-\mathbf{k}|}^c \tag{14a}$$

and

$$V_{\mathbf{q},\mathbf{k}}^{(1)} = n_f S_q^c \left[\frac{\mathbf{q} \cdot \mathbf{k}}{q^2} \hat{c}_k^c + \frac{\mathbf{q} \cdot (\mathbf{q} - \mathbf{k})}{q^2} \frac{1}{n_f} \right]^2 S_k^c S_{|\mathbf{q}-\mathbf{k}|}^b, \quad (14b)$$

where $\hat{c}_q^c$, the Fourier transform of the connected direct correlation function, has been introduced.

Based on these equations, a few general comments are in order. First of all, the derived expressions retain the mathematical structure of the typical mode-coupling equations which have been extensively studied in Ref. [18]. Thus, all known properties of the solutions of MCT equations, in particular near the transition, apply in the case of the QA mixture. A significant addition compared to the bulk is however the presence of a linear term in the memory function, which opens the possibility of continuous ideal glass transitions.

Like in the theory for the bulk, which is recovered in the limit $n_m \to 0$, the slow dynamics is fully determined by smoothly varying static quantities. Interestingly, no explicit reference to the matrix is visible in the equations. Indeed, the only required information is n_f, S_q^c, S_q^b, and $\hat{c}_q^c$, i.e., quantities characterizing the fluid component of the QA system. These functions and the relations between them are generically meaningful for the description of fluids evolving in statistically homogeneous random environments and they are by no means restricted to the model of the QA mixture (for the case of nonparticle-based random fields, see Refs. [39,40]). Therefore, one can expect that the present dynamical theory shares the same degree of generality and is applicable in its present form out of the strict context of the QA binary mixture. In fact, this shows up nicely in the process of deriving the equations, since one finds that the contributions resulting from the coupling of the random forces to $\delta\rho_{\mathbf{k}}^f \rho_{\mathbf{q}-\mathbf{k}}^m$ are identically zero (see Appendix B). Thus it is enough to consider only two types of quadratic variables, $\delta\rho_{\mathbf{k}}^f \delta\rho_{\mathbf{q}-\mathbf{k}}^f$ and $\delta\rho_{\mathbf{k}}^f \langle\rho_{\mathbf{q}-\mathbf{k}}^f\rangle$, precisely those which are not specific to QA systems, to obtain the same dynamical equations. Further evidence of the generic character of the present equations is given in Appendix C, where the dynamics of a mean-field spin-glass model in a random magnetic field is shown to obey equations with exactly the same structure.

Along the same line, it is noteworthy that the total fluid structure factor S_q^{ff} does not appear in the derived dynamical equations. Only S_q^c and S_q^b do. It results that, in the framework of the MCT, the global fluid correlations are of limited relevance to discuss the relation between the statics and the dynamics. A much more important aspect is rather the balance between the connected and disconnected contributions to these correlations. This result is very welcome, since similar differences in the roles played by these three types of correlations are known to be crucial in the physics of QA systems. This is best illustrated by the compressibility sum rule [11,15], which precisely involves S_q^c and not S_q^{ff}, as one would naively expect from the relation for the bulk. It is thus reassuring that this feature has been preserved despite the uncontrolled approximations involved in the derivation of the theory. Moreover, this finding allows one to clarify the issues raised in Refs. [25,27] about the possibility of a description of the dynamics in confinement with theories based on structural quantities only. Indeed, it was observed there that systems with identical global fluid correlations could

have significantly different dynamics, a result which appeared as a challenge to such approaches. The present MCT shows that this is not necessarily so and that one should also consider the connected and blocked correlations before a conclusion can be reached.

About the form of the vertices, one can note the familiar expression of $V_{\mathbf{q},\mathbf{k}}^{(2)}$, which measures the coupling of the random forces to $\delta\rho_{\mathbf{k}}^f \delta\rho_{\mathbf{q}-\mathbf{k}}^f$. It is the same as in a bulk system, with connected quantities simply replacing the fluid structure factor and direct correlation function. This is true for Ω_q^2, given by Eq. (12), as well. Thus we find that the relaxing part of the density fluctuations in a QA system just behaves dynamically like the corresponding degree of freedom in the bulk. This is not really surprising, since a similar correspondence is already visible in the statics, for instance in the OZ equation (A3c) or in the convolution approximation (B6a), which are both used in the calculation of $V_{\mathbf{q},\mathbf{k}}^{(2)}$. Such a correspondence was missing in all our attempts to derive a MCT starting from the total density fluctuations and this is one of the reasons for which the resulting equations were considered unsatisfactory. $V_{\mathbf{q},\mathbf{k}}^{(1)}$ is less obvious and combines features of $V_{\mathbf{q},\mathbf{k}}^{(2)}$ and of the vertex for the tagged particle dynamics in the bulk [18]. In particular, like the latter, it diverges when $q \to 0$.

Finally, the above equations differ slightly from those reported in Ref. [37], where a first account of the theory was given. There, $S_{|\mathbf{q}-\mathbf{k}|}^b$ in Eq. (14b) is replaced by $S_{|\mathbf{q}-\mathbf{k}|}^b - n_f \hat{c}_{|\mathbf{q}-\mathbf{k}|}^b (S_{|\mathbf{q}-\mathbf{k}|}^c)^2$, where $\hat{c}_q^b$ is the Fourier transform of the blocked direct correlation function. The only difference between the two approaches is that $\delta\rho_{\mathbf{k}}^f \langle\rho_{\mathbf{q}-\mathbf{k}}^f\rangle$ was not included as a slow variable in the earlier mode-coupling scheme. *A priori*, this is an unjustified approximation. Indeed, as shown in Appendix B, the coupling to this variable is actually so strong, that, when both $\delta\rho_{\mathbf{k}}^f \rho_{\mathbf{q}-\mathbf{k}}^m$ and $\delta\rho_{\mathbf{k}}^f \langle\rho_{\mathbf{q}-\mathbf{k}}^f\rangle$ are considered, the contribution of the former becomes identically zero, while the effect of the random environment is integrally transferred to the latter. There are nevertheless circumstances in which the absence of $\delta\rho_{\mathbf{k}}^f \langle\rho_{\mathbf{q}-\mathbf{k}}^f\rangle$ looks perfectly well motivated, for instance when a single particle is moving in the porous matrix, corresponding to the limit $n_f \to 0$, or when the adsorbed fluid is an ideal gas [41]. In both cases, the present MCT reduces to $\Omega_q^2 = q^2 k_B T / m$ and

$$m_q^{(MC)}(t) = \int \frac{d^3\mathbf{k}}{(2\pi)^3} \left[\frac{\mathbf{q} \cdot (\mathbf{q} - \mathbf{k})}{q^2} \right]^2 \hat{h}_{|\mathbf{q}-\mathbf{k}|}^b \phi_k(t), \quad (15)$$

where $\hat{h}_q^b$ is the Fourier transform of the blocked total pair correlation function. But, since the only forces exerted on the fluid are those due to the random matrix, on physical grounds, the only mode-coupling contributions to the relaxation kernel are expected to come from $\delta\rho_{\mathbf{k}}^f \rho_{\mathbf{q}-\mathbf{k}}^m$. All previous theories of the Lorentz gas have been based on this insight, which leads to the same equations as above, except that $\hat{h}_{|\mathbf{q}-\mathbf{k}|}^b$ in Eq. (15) is replaced with $\hat{h}_{|\mathbf{q}-\mathbf{k}|}^b - \hat{c}_{|\mathbf{q}-\mathbf{k}|}^b$ [29–31]. Note that, for an adsorbed ideal gas, both theories correctly predict that the dynamics is independent of n_f.

It seems thus that there is a subtle interplay between the approximations involved in the derivation of the MCT and

the peculiar structure of the static correlations in the QA mixture. At present, it is not clear what to conclude from this observation, but it is interesting that the difference between the two MCT schemes involves the blocked direct correlation function [42]. Indeed, this is a rather delicate object, not easily captured by simple approximations. This is best understood in the replica framework, where $c^b(r)$ is obtained as the zero replica limit of the direct correlation function between two noninteracting fluid replicas only correlated through their common interaction with the matrix [12–15]. It results that $c^b(r)$ has a highly nonadditive character and that, for instance, most simple closures of the replica OZ equations fail to provide expressions for this function which do not vanish identically. Thus, it is a rather nontrivial finding that the MCT approximation scheme is actually sensitive to the existence of this function.

III. SELF-INDUCED GLASSINESS VERSUS QUENCHED RANDOM ENVIRONMENT

From the previous discussion, it is clear that the separation of the fluid density fluctuations into relaxing and frozen parts plays a crucial role in the derivation of the MCT for QA systems. In that case, the freezing is of static origin, due to the random external field generated by the quenched matrix. But, as it is well known from the MCT for bulk fluids, freezing of the density fluctuations may also occur dynamically, when the system enters in the ideal glassy state. It seems thus interesting to compare both situations. This can be seen as a case of self-induced versus quenched disorder, similar to what has been discussed many times in the literature [43–46].

The residual relaxation of a bulk fluid in its ideal glassy state has been studied in Ref. [47]. It is described by mode-coupling equations of the same form as above, except that the characteristic frequency is given by

$$\Omega_q^2 = \frac{q^2 k_B T}{m\{(1-f_q)S_q\}}, \tag{16}$$

and the vertices are

$$V_{\mathbf{q},\mathbf{k}}^{(2)} = \frac{1}{2}n_f\{(1-f_q)S_q\}\left[\frac{\mathbf{q}\cdot\mathbf{k}}{q^2}\hat{c}_k + \frac{\mathbf{q}\cdot(\mathbf{q}-\mathbf{k})}{q^2}\hat{c}_{|\mathbf{q}-\mathbf{k}|}\right]^2$$
$$\times\{(1-f_k)S_k\}\{(1-f_{|\mathbf{q}-\mathbf{k}|})S_{|\mathbf{q}-\mathbf{k}|}\} \tag{17a}$$

and

$$V_{\mathbf{q},\mathbf{k}}^{(1)} = n_f\{(1-f_q)S_q\}\left[\frac{\mathbf{q}\cdot\mathbf{k}}{q^2}\hat{c}_k + \frac{\mathbf{q}\cdot(\mathbf{q}-\mathbf{k})}{q^2}\hat{c}_{|\mathbf{q}-\mathbf{k}|}\right]^2$$
$$\times\{(1-f_k)S_k\}\{f_{|\mathbf{q}-\mathbf{k}|}S_{|\mathbf{q}-\mathbf{k}|}\}, \tag{17b}$$

where n_f is the density of the fluid, S_q its structure factor, $\hat{c}_q$ the Fourier transform of its direct correlation function, and f_q the Debye-Waller factor of the glass. Accordingly, $f_q S_q$ corresponds to the dynamically frozen part of the density fluctuations, while $(1-f_q)S_q$ corresponds to their relaxing part.

The analogies between these equations and Eqs. (12) and (14) are striking. There is almost a perfect correspondence

between $(1-f_q)S_q$ and S_q^c on the one hand, and $f_q S_q$ and S_q^b on the other hand. Thus, we find that, irrespective of the mechanism of freezing of the fluid density fluctuations, the resulting relaxing and frozen contributions essentially play the same role in both systems.

But there remains one significant difference between both sets of equations. Indeed, one of the Fourier transformed direct correlation functions in Eq. (17b), the one which carries the same wave vector as the frozen part of the structure factor, is replaced by a simple constant factor $1/n_f$ in Eq. (14b). The origin of this constant term should probably be traced back to the asymmetric nature of the QA system, where the fluid reacts to the matrix but not the other way around, resulting in a nonequilibrium character of its static and dynamical correlations, in the sense that the matrix is not equilibrated with the fluid. It would then reflect the lack of dynamical self-consistency between the glassy dynamics in a QA system and the frozen background on top of which it develops.

It is tempting to try and obtain the MCT for the QA binary mixture as a limiting case of the MCT for the ordinary binary mixture [48], where one component would become the quenched matrix. The above discussion shows that this is not possible. Indeed, based on heuristic considerations, one can get close to Eqs. (16) and (17), for instance by canceling all terms which would result in a time dependence of the fluid-matrix and matrix-matrix correlations, but the nonequilibrium density factor identified above seems impossible to generate from the theory for the fully annealed system. Thus, as far as the development of theoretical approaches is concerned, and this statement is probably not restricted to the MCT framework, the dynamics of a QA system should definitely be considered from the start as different from an infinite mass (for Newtonian systems) or a zero bare diffusivity (for Brownian dynamics) limit of the dynamics of a fully annealed mixture. This is actually not so unexpected since, already in the statics, similar difficulties were met in early attempts to derive the equations valid for the QA mixture starting from those describing fully equilibrated systems (see the discussion of Refs. [9,10,49] in Ref. [14]).

Thus the present theory is not a special case of earlier mode-coupling studies of the dynamics of particles moving in a glassy matrix [50]. There, the MCT for binary mixtures was used in a regime where one component, made of big particles, was completely glassy, i.e., both the collective and tagged particle correlators did not relax to zero, while the other component, made of small spheres, was not necessarily localized, i.e., the tagged particle correlators could relax to zero. In fact, both theories are complementary. In the early approach, the glassy matrix has to be the product of the self-consistent mode-coupling dynamics, but the model incorporates thermal fluctuations of the solid and aspects of its response to the presence of the fluid, while in the present approach, one has much more freedom to choose the structure of the confining medium, including realistic models of porous solids [51], but the disordered matrix is rigorously inert. There are anyway qualitative analogies between both models. For instance, there is a clear link between the fact that the collective motion of the small particles in a binary mixture necessarily becomes nonergodic at the same point as

that of the big particles and the unavoidable existence of static blocked correlations for a fluid in a random matrix.

IV. DYNAMICAL PHASE DIAGRAMS

We now move to the quantitative predictions of the theory, which require numerical solutions of the MCT equations. In this section, we report dynamical phase diagrams, obtained by mapping, in the parameter space of a given model, the domain where $\lim_{t\to\infty}\phi_q(t)=0$, corresponding to the ergodic fluid phase, and the one where $\lim_{t\to\infty}\phi_q(t)=f_q \neq 0$, corresponding to the nonergodic ideal glassy state. The interface between the two domains forms the ideal liquid-glass transition manifold; in the present work, it will always be a line, since only systems with a two-dimensional parameter space are considered. Details of the dynamical changes when crossing this line are discussed in the next section.

As already mentioned in Sec. II, a significant difference between the MCT equations for QA systems and those for bulk glass formers is the presence of a linear term in the memory kernel (13). It results that the discontinuous or type B transition scenario known from the bulk, where the infinite time limit of $\phi_q(t)$ jumps discontinuously from zero to a finite value when going from the liquid to the glass, is not the only possibility anymore. Continuous or type A transition scenarios, where f_q grows continuously from zero when entering the glassy phase, indeed become possible.

This is best understood by reference to the so-called F_{1n} ($n\geq 2$) schematic models [18], in which the time evolution of a single correlation function $\phi(t)$ is ruled by a two parameter memory kernel of the form

$$m_{1n}(t) = v_1\phi(t) + v_n\phi(t)^n, \quad v_1, v_n \geq 0. \quad (18)$$

It can be readily shown that, when the second term dominates (v_1 small), these models have a line of type B transitions starting at $v_1=0, v_n=n^n/(n-1)^{n-1}$, and, when the first term dominates (v_n small), they have a line of type A transitions starting at $v_1=1, v_n=0$. The study of the F_{1n} models also gives us information on the possible topologies of the dynamical phase diagrams, which depend on the way the transition lines meet. Two simple cases are found [18]. If $n=2$, the two lines join smoothly at a common endpoint, where a topologically stable degenerate A_3 singularity is located. If $n>2$, the two lines intersect and, in the glassy domain, only the extension of the type B transition line subsists beyond the intersection, forming a glass-glass transition line terminated by an ordinary A_3 singularity.

It turns out that these two prototypical shapes of phase diagrams are obtained with two very simple, closely related QA mixture models, to which the present study is restricted. In both, the fluid-fluid and fluid-matrix interactions are pure hard core repulsions of the same diameter d. The only difference lies in the matrix correlations. In model I, the matrix configurations are assumed to be quenched from an equilibrium fluid of hard spheres of diameter d, so that the matrix particles do not overlap, while in model II the matrix particles are completely uncorrelated and overlap freely. In the following, both systems will be parametrized by the two dimensionless densities $\phi_f=\pi n_f d^3/6$ and $\phi_m=\pi n_m d^3/6$, and

the Percus-Yevick (PY) approximation [12–14,52] will be used to compute the required structural quantities. Note that, in this approximation, $c^b(r)\equiv 0$, so that the difficulties mentioned at the end of Sec. II are irrelevant.

The nonergodicity parameter f_q is a solution of the nonlinear set of equations

$$\frac{f_q}{1-f_q} = \int \frac{d^3\mathbf{k}}{(2\pi)^3}\left[V_{\mathbf{q},\mathbf{k}}^{(2)}f_kf_{|\mathbf{q}-\mathbf{k}|} + V_{\mathbf{q},\mathbf{k}}^{(1)}f_k\right], \quad (19)$$

which has to be solved numerically in order to locate the liquid and glassy phases when ϕ_f and ϕ_m are varied. All computations in the present work have been achieved using the method of Ref. [53], to which the interested reader is referred for technical details, and we only provide the quantitative information needed to reproduce the present results, i.e., that the wave vector integrals have been discretized to points on a grid of 128 equally spaced values with step size $\Delta\simeq 0.3835/d$, starting at $q_{min}=\Delta/2$ [54]. We have checked by two means that this discretization is not too coarse, in particular with respect to the small q divergence of the memory kernel which is cut off. First, test calculations at various fluid and matrix densities have been performed on a finer q grid, hence with a smaller q_{min}. Second, in the $n_f \to 0$ limit, we have compared our prediction for the diffusion-localization point of model I with Leutheusser's analytic result obtained within an additional hydrodynamic approximation which allows to integrate exactly over the full q range [30]. In all cases, only modest quantitative differences of a few percents on the location of the transition points were found.

When dealing with complex transition scenarios, including higher-order singularities and glass-glass transition lines, a useful quantity to consider is the largest eigenvalue E of the stability matrix of the set of equations (19). Indeed, there holds $E\leq 1$, and E goes to 1 when a transition is approached from the strong coupling side [55]. Thus, $1-E$ can be used as a convergence criterion for the determination of the transition points [56]. In this work, $1-E\leq 10^{-3}$ was assured for ordinary transition points and $1-E\leq 10^{-5}$ was required in the regions where the transition lines of types A and B meet.

The dynamical phase diagrams of models I and II are reported in Fig. 2. In the left panel, they are plotted in the (ϕ_m, ϕ_f) plane. This is the obvious parameter space of the problem, but, with this choice of variables, no account is given of the differences in structure between the two matrix models. This clearly limits the possibilities of a meaningful comparison between the two systems. Thus, in the right panel, both QA mixtures have been tentatively parametrized by the same physical constant, their Henry constant $K_H(\phi_m)$. For systems with hard core interactions, $K_H(\phi_m)$ is equal to the fraction of the total volume accessible to the center of an adsorbate particle in a matrix of density ϕ_m and is probably the most simple and generic scalar quantity characterizing the confining effect of a solid matrix on an adsorbed fluid. It is given by $\exp(-8\phi_m)$ for model II [57], and by $\exp[-\beta\mu_{ex}(\phi_m)]$ for model I, where $\mu_{ex}(\phi_m)$ is the excess chemical potential of the equilibrium hard sphere fluid with
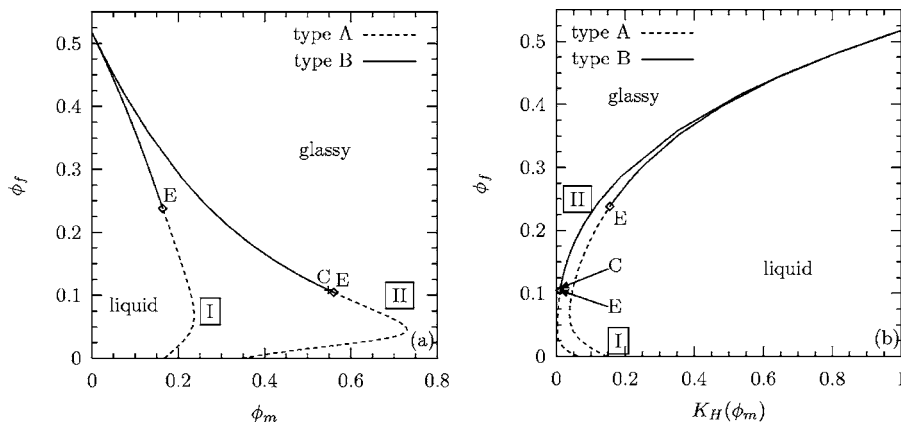
FIG. 2. Dynamical phase diagrams of two types of hard sphere quenched-annealed binary mixtures. (a) In the (ϕ_m, ϕ_f) plane. (b) In the $[K_H(\phi_m), \phi_f]$ plane. Model I: Nonoverlapping matrix particles. Model II: Freely overlapping matrix particles. The A_3 singularities are indicated with diamonds and denoted by E, while the crossing point between the type A and B transition lines in model II is indicated by a cross and denoted by C.

volume fraction ϕ_m [58]. The latter has been estimated following the compressibility route within the PY approximation [59].

As it can be readily seen in Fig. 2, both phase diagrams essentially have the same overall shape, especially when they are plotted as functions of $K_H(\phi_m)$. Their main qualitative difference at this global scale, which is the difference in concavity of their upper parts visible in Fig. 2(a), turns out to be rather insignificant, as it is the simple and direct consequence of the fact that the strength of confinement increases more slowly with ϕ_m in model II than in model I, because of the overlapping matrix particles. It completely disappears in Fig. 2(b).

The nature of the ideal glass transitions met in the phase diagrams is just as expected from the study of schematic models. Starting from the type B liquid-glass transition point for the bulk (at $\phi_m=0$), where the memory kernel is purely quadratic, a line of type B transitions develops when increasing ϕ_m, and, starting from the type A diffusion-localization point (at $\phi_f=0$), where the memory kernel is purely linear, a line of type A transitions emerges when increasing ϕ_f. The same is true of the way the two lines meet in the phase diagrams. On the one hand, for model I, the type A and B lines have a common end point, denoted by E, where they smoothly join and form a degenerate A_3 singularity, like in the F_{12} model. On the other hand, for model II, the two lines intersect at a crossing point C and the extension of the type B transition line in the glassy domain becomes a glass-glass transition line ending with an ordinary A_3 singularity, denoted by E as well. This is the scenario obtained with the F_{1n} models, for $n>2$. Note that, to our knowledge, this is the first time that these widely studied one equation toy models find physical realizations as fluid systems.

The glass-glass transition line of model II, located between points C and E, is barely visible at the scale of Fig. 2. It is short and not well separated from the type A liquid-glass transition line. Taking into account the idealized nature of the predictions of the MCT, it would probably be impossible to detect it unambiguously in computer simulations of this system. Only the very specific features of the dynamics in the vicinity of a higher-order singularity, be it degenerate or not, should be visible, like logarithmic decay laws and subdiffusive behaviors [18,21,56,60]. But, at least, the present calculation shows that this scenario can actually be realized and that this does not require any exotic physical ingredient.

Now that a suitable starting point is available, by playing with the parameters of the model, one can try and obtain a system for which this glass-glass transition line would be extended enough for its signatures to be observable in simulations.

A final requirement for a complete characterization of the transitions studied in this work is the knowledge of the so-called exponent parameter λ [18]. It determines many aspects of the dynamics near a transition (see the next section) and, for this reason, plays a crucial role in the theory. One has $0 \le \lambda \le 1$ and $1/2 \le \lambda \le 1$ for type A and B transitions, respectively. Also, λ reaches 1, its maximum value, at end point singularities and jumps discontinuously at crossing points. This is thus a useful parameter to follow during the computation of the phase diagrams. It is plotted in Fig. 3 as a function of ϕ_f at the transition. For model II, points C_1 and C_2 mark the discontinuity associated with the crossing point C in Fig. 2 and the existence of glass-glass transitions is clearly visible, with values of λ given by the line between points C_1 and E. For the same model, a nonmonotonic variation of λ along the type B line can be noted as well.

In addition to these transition scenarios, and formally not related to them, another remarkable prediction of the present
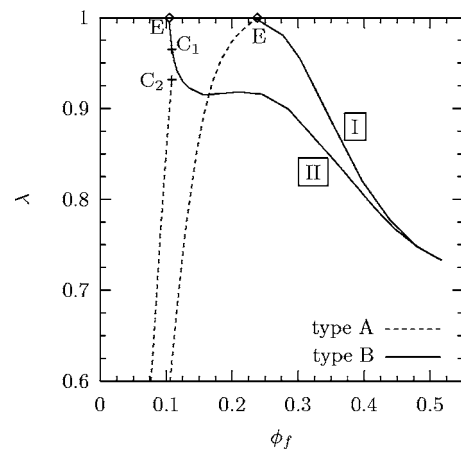

FIG. 3. Exponent parameter λ along the transition lines of models I and II. The lowest part, where λ goes to zero with ϕ_f, has been omitted for readability. For both models, E denotes the A_3 singularity, with $\lambda=1$. C_1 and C_2 delimit the discontinuity associated with the crossing point between the type A and B transition lines in model II.

theory is a reentry phenomenon for matrix densities higher than the localization threshold (obtained for $\phi_f=0$). Indeed, as shown in Fig. 2(a), for a given, not too high ϕ_m in this domain, ergodicity can be broken either by an increase or a decrease of the fluid density.

In hard core systems, freezing by an increase of the fluid density can be qualitatively understood from simple free volume arguments, which provide a direct explanation for the decrease of ϕ_f at the transition as a function of ϕ_m in the upper part of the phase diagrams. Because of the volume excluded by the matrix particles, the larger the matrix density is, the smaller the fluid density has to be for structural arrest to occur. From the results for model I, we might further note that this decrease is such that the total compacity $\phi_f+\phi_m$ at the transition is a decreasing function of ϕ_m as well, reflecting the fact that the inclusion of immobile matrix particles in the system slows down the dynamics more efficiently than the inclusion of the same amount of mobile fluid particles. Such a behavior, which is hardly surprising, has already been observed in molecular dynamics simulations [26,27].

The possibility of an ergodicity breaking transition by a decrease of the fluid density, which is reflected in the bottom part of the phase diagrams by the increase with ϕ_m of the transition ϕ_f, is more unexpected. We interpret this prediction as the signature of a delocalization phenomenon induced by fluid-fluid interactions. More precisely, we propose that the occasional collisions between the fluid particles at low ϕ_f can destroy the dynamical correlations responsible for the localization of individual particles in dense enough matrices. For this process to provide an efficient ergodicity restoring relaxation channel, a reasonable criterion is that the localization domains should overlap to allow the fluid particles to interact. Thus the localization length computed at $\phi_f=0$, which decreases when ϕ_m increases, should be comparable to the average distance between two fluid particles, which decreases when ϕ_f increases. It is then immediate that, starting in the localized state, the larger ϕ_m is, the higher ϕ_f has to be in order to restore ergodicity. The physical implications of this result will be discussed in more detail in the last section.

Dynamical scenarios involving reentrant glass transition lines, higher-order singularities, and glass-glass transition lines, have already been found for colloidal suspensions with short-ranged attractions [21]. By analyzing various contributions to the memory kernel, these features were shown to result from the interplay of two well defined phenomena, cage effect and bond formation, driven by the hard core and attractive parts of the interaction, respectively. It seems thus interesting to attempt such an analysis for the present problem.

Guided by the results of Sec. III, we propose that a contribution represented by a memory kernel $m_q^{(cage)}(t)$ derived from $m_q^{(MC)}(t)$ by replacing $1/n_f$ in Eq. (14b) with $\hat{c}_{|\mathbf{q}-\mathbf{k}|}^c$ should be isolated. Indeed, the resulting expression then coincides with the one describing the residual dynamics of a bulk ideal glass. Therefore, one can reasonably expect that, for a QA system, $m_q^{(cage)}(t)$ will provide a fair representation of the mechanism of caging by fluid particles in the presence of permanent density fluctuations, which is precisely the one
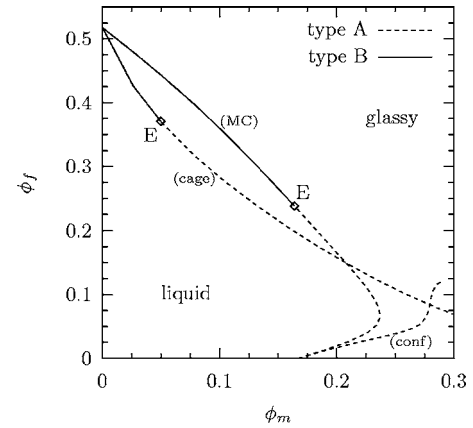

FIG. 4. Real and hypothetical dynamical phase diagrams of model I, computed with the total and partial memory kernels $m_q^{(MC)}(t)$, $m_q^{(cage)}(t)$, and $m_q^{(conf)}(t)$. The curves are labeled accordingly and the degenerate A_3 singularities are denoted by E.

at work in bulk glassy systems. The remaining linear kernel $m_q^{(conf)}(t)=m_q^{(MC)}(t)-m_q^{(cage)}(t)$ can then be attributed to the confinement-specific phenomena, i.e., the localization effect of the matrix combined with the unusual decorrelation mechanism due to fluid-fluid collisions discussed above. In principle, one could try to separate these two processes, using the fact that, for an ideal gas, only the localization effect is present and leads to a matrix density at the transition which is independent of the fluid density. However, already with the present limited separation, the somewhat artificial character of the procedure shows up in the form of negative values of $m_q^{(conf)}(t)$, which restrict the density domain where stable solutions of the MCT equations can be found, so no further decomposition of $m_q^{(conf)}(t)$ was attempted.

The hypothetical phase diagrams computed with the partial kernels $m_q^{(cage)}(t)$ and $m_q^{(conf)}(t)$ for model I are reported in Fig. 4, where they are compared to the one obtained with the full $m_q^{(MC)}(t)$. Clearly, the reentry phenomenon observed in the complete phase diagram can be explained by the interplay of the two contributions discussed above. But, at variance with the colloidal systems, the higher-order singularity is not located in the domain where they cross over. The interpretation of this finding is ambiguous. On the one hand, since a higher-order singularity is found on the transition line computed with $m_q^{(cage)}(t)$ as well, one might argue that the singularity should be considered as an integral part of the scenario of caging by fluid particles. Then, in the relevant domain, confinement would simply appear as a modifier of the cage structure, progressively changing the nature of the ideal jamming transition from discontinuous to continuous. On the other hand, the bifurcation analysis of the MCT scenario shows that a higher-order singularity is necessarily formed when two lines of type A and B transitions meet. Then, since the type A and B lines arise from points representative of systems ruled by confinement and bulk caging, respectively, one might consider that the singularity is the product of the interplay of these two phenomena. In favor of the latter interpretation, it has been recently suggested that higher-order singularities generically result from a competi-
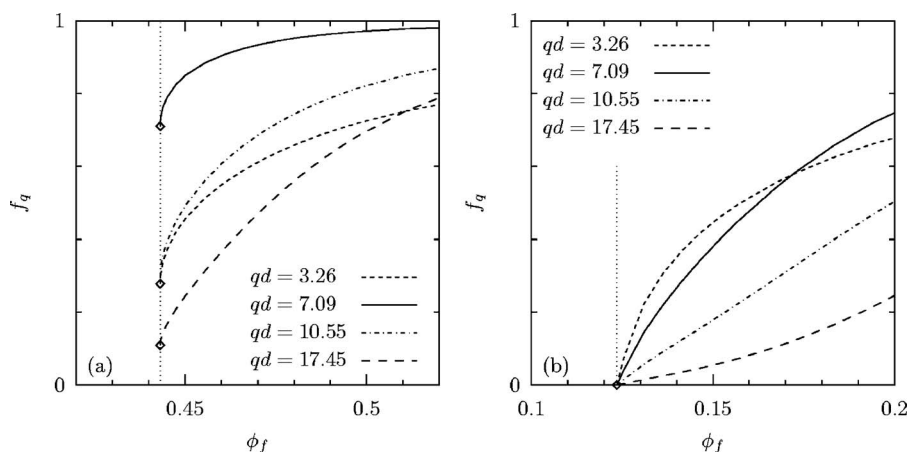
FIG. 5. Fluid density dependence of the nonergodicity parameter $f_q = \lim_{t \to \infty} \phi_q(t)$ for model I at two matrix densities. (a) Type B transition for $\phi_m = 0.05$. (b) Type A transition for $\phi_m = 0.22$. Data for four representative wave vectors are shown. Vertical dotted lines and diamonds indicate the ideal glass transition.

tion between different arrest mechanisms [61]. Note however that the conclusions of Ref. [61] are drawn from the consideration of bulk systems only, which necessarily enter into the glassy state through type B transitions and for which there is no mathematical constraint in the theory imposing *a priori* the existence of a singularity. It is not immediate that the proposed statement is valid or even needed for systems where type A and B liquid-glass transitions coexist.

V. TYPICAL TRANSITION SCENARIOS

It results from the previous section that, if one stays away from the higher-order singularities, the crossing points, and the glass-glass transitions, which require fine-tuning of the parameters of the models, the present MCT for QA mixtures predicts two generic liquid-glass transition scenarios. One is discontinuous or type B, the other is continuous or type A. In this section, we discuss the different features of these transitions which are relevant for comparisons of experimental or simulation data with the predictions of the theory. The analytic results will be quoted without their proofs, which can be found in Ref. [18]. They will be illustrated with detailed computations for model I at two matrix densities, $\phi_m = 0.05$ and $\phi_m = 0.22$. For the former value, a type B transition occurs at $\phi_f^c \simeq 0.443$, with $\lambda \simeq 0.774$. For the latter, a type A transition is found at $\phi_f^c \simeq 0.124$, with $\lambda \simeq 0.729$. For this matrix density, we consider the type A transition on the upper branch of the phase diagram, as it is of greater relevance for the problem of the glass transition in confinement. In both cases, keeping $\lambda \leq 0.8$ allows one to consider that the transitions are far enough from the higher-order singularity.

Here, a comment on the method of solution of the mode-coupling equations is in order. Indeed, as mentioned in the previous section, it involves a cutoff of the low q divergence of the memory kernel. Since it has been demonstrated that this divergence can change the qualitative properties of the solutions in the asymptotic regime near the transition [33,62,63], this approximation and the use of the results of Ref. [18], which have been obtained under the assumption of nonsingular vertices, might look problematic. In fact, this is not the case for physical reasons. Indeed, in the Lorentz gas limit, the low q singularity of the memory function has been shown to be an ill feature of the mode-coupling approxima-

tion [62]. Thus, from a physical point of view, the discretized equations considered in the present calculation are actually more satisfactory than the continuous ones and the results reviewed in Ref. [18] can legitimately be applied.

We first consider the density dependence of the nonergodicity parameter f_q, shown in Fig. 5. As it should, f_q takes a finite value at the ideal glass transition point of type B, while it grows continuously from zero at the type A transition. In the glassy state, the bifurcation analysis of Eq. (19) to leading order yields two universal power law behaviors,

$$f_q - f_q^c \propto (\phi_f - \phi_f^c)^{1/2} \qquad (20)$$

for a type B scenario, and

$$f_q \propto (\phi_f - \phi_f^c) \qquad (21)$$

near a type A transition. Accordingly, in Fig. 5, the curves corresponding to the type B and A transitions start with infinite and finite slopes, respectively.

The wave vector dependence of f_q, though not universal, is an important prediction of the MCT as well. It is reported in Fig. 6. In Fig. 6(a), f_q is shown at the type B transition, while in Fig. 6(b), since $f_q^c = 0$ at a type A transition, the results at $\phi_f = 1.1 \phi_f^c$ are plotted. For reference, the two relevant structure factors S_q^c and S_q^b at ϕ_f^c are also given. Note that in both cases, S_q^b shows maxima both where S_q^c has maxima or minima. At the type B transition, except for the peak at $q=0$ where f_q reaches 1 as a consequence of the diverging kernel, the nonergodicity parameter is very similar to the one found for a bulk hard sphere fluid and oscillates with S_q^c, which precisely represents bulklike correlations. The overall amplitude is smaller than in the bulk, reflecting the fact that, when ϕ_m increases, the system evolves towards a continuous transition scenario. In comparison, the nonergodicity parameter near the type A transition appears rather featureless. f_q simply decreases from 1 at $q=0$, with, as ϕ_f is increased, a small shoulder developing in the wave vector regime where S_q^c has its main peak and S_q^b its second peak. With the present models where the fluid and matrix particles have the same size, it is not clear which changes in the static correlations are actually responsible for the growth of this contribution.

Beside these results for the infinite time limit of the density correlation functions, the full dynamics is of great inter-
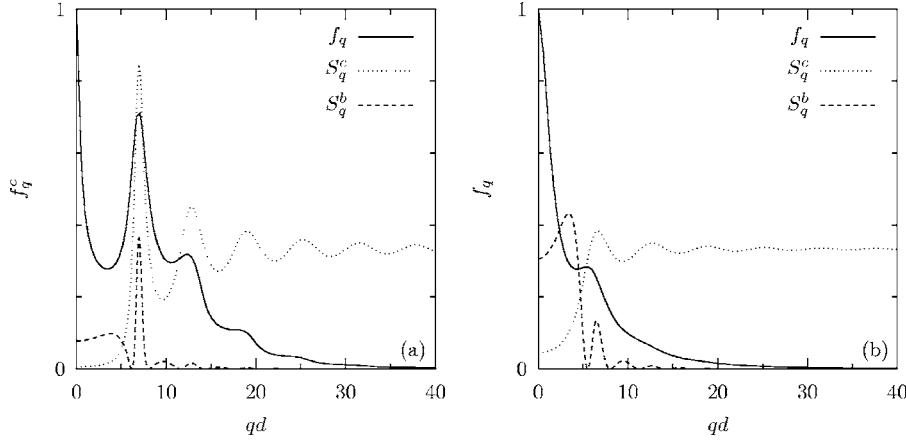
FIG. 6. Wave vector dependence of the nonergodicity parameter $f_q = \lim_{t\to\infty} \phi_q(t)$ for model I at two matrix and fluid densities. (a) At the type B transition for $\phi_m = 0.05$. (b) Near the type A transition for $\phi_m = 0.22$, at $\phi_f = 1.1\phi_f^c$. In both panels, S_q^c and S_q^b at ϕ_f^c are reported for reference (S_q^c has been divided by 3 for readability).

est as well. For this computation, which uses the algorithm described in Ref. [64], we follow Ref. [53] and reduce the generalized Langevin equation (11) to its form valid for Brownian dynamics,

$$\tau_q \dot{\phi}_q(t) + \phi_q(t) + \int_0^t d\tau\, m_q(t-\tau)\dot{\phi}_q(\tau) = 0, \qquad (22)$$

with

$$\tau_q = t_{\mathrm{mic}} S_q^c / (qd)^2 \qquad (23)$$

and the initial condition $\phi_q(0) = 1$. This simplification affects the short time transient part of the dynamics, but not its long time properties. In the following, the unit of time shall be chosen such that $t_{\mathrm{mic}} = 160$.

The time evolution of the density correlation function $\phi_q(t)$ at $q \simeq 7.09/d$, corresponding to the main peak of S_q^c, is reported in Fig. 7 for state points in the vicinity of the two transitions discussed above. The curves for other values of q are qualitatively similar. In Fig. 7(a), the two step dynamics typical of the discontinuous ideal glass transition scenario and well known from the study of bulk systems is easily recognized in the curves corresponding to the liquid state.

The second step, associated to the decay from the plateau where $\phi_q(t) \simeq f_q^c$, obeys the so-called superposition principle, which states that, in this regime and for a given q, the shape of the dynamics is independent of the state point. The relaxation functions only differ through the characteristic time scale τ_α, which displays a power law divergence,

$$\tau_\alpha \propto (\phi_f - \phi_f^c)^{-\gamma}, \qquad (24)$$

when the transition is approached. One shows that

$$\gamma = \frac{1}{2a} + \frac{1}{2b}, \qquad (25)$$

where the exponents a and b ($0 < a < 1/2, b > 0$) are related to λ through

$$\frac{\Gamma(1-a)^2}{\Gamma(1-2a)} = \frac{\Gamma(1+b)^2}{\Gamma(1+2b)} = \lambda, \qquad (26)$$

Γ denoting Euler's gamma function. In the glassy state, only the first relaxation step remains and, when t goes to infinity, $\phi_q(t)$ reaches f_q, which increases with ϕ_f as shown in Fig. 5(a).
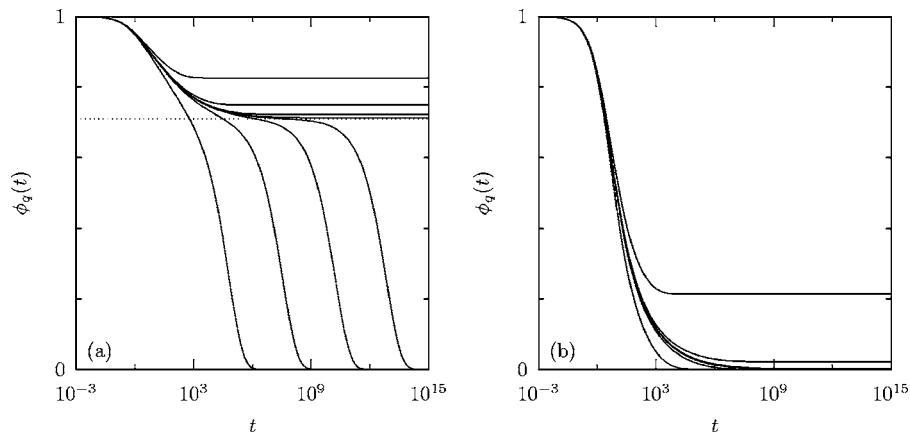

FIG. 7. Time evolution of the connected density correlation function $\phi_q(t)$ at $q \simeq 7.09/d$ for model I at two matrix densities. (a) In the vicinity of the type B transition for $\phi_m = 0.05$; from left to right, bottom to top: $\phi_f = 0.99\phi_f^c$, $0.999\phi_f^c$, $0.9999\phi_f^c$, $0.99999\phi_f^c$, $1.00001\phi_f^c$, $1.0001\phi_f^c$, $1.001\phi_f^c$, and $1.01\phi_f^c$. The horizontal dotted line marks f_q^c, the nonergodicity parameter at the transition. (b) In the vicinity of the type A transition for $\phi_m = 0.22$; from left to right, bottom to top: $\phi_f = 0.9\phi_f^c$, $0.99\phi_f^c$, $0.999\phi_f^c$, $0.9999\phi_f^c$, $1.0001\phi_f^c$, $1.001\phi_f^c$, $1.01\phi_f^c$, and $1.1\phi_f^c$.
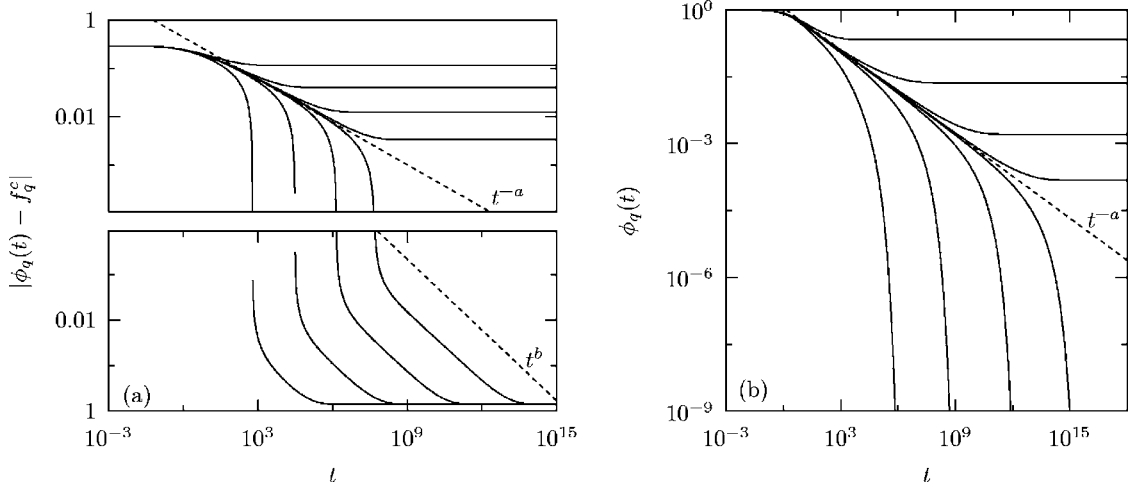
FIG. 8. Critical dynamics of the connected density correlation function $\phi_q(t)$ at $q \simeq 7.09/d$ for model I at two matrix densities. (a) In the vicinity of the type B transition for $\phi_m = 0.05$. As it should, only the data for $\phi_f < \phi_f^c$ appear in the bottom panel (note its reverted y scale, in order to make it graphically clear that, despite the use of the absolute value, a decay law is represented). (b) In the vicinity of the type A transition for $\phi_m = 0.22$. See Fig. 7 for attribution of the curves. The analytically derived power law behaviors (32) and (33) are shown as dashed straight lines.

The dynamics near the type A transition visible in Fig. 7(b) looks significantly different, with a single step relaxation scenario, both in the liquid and glassy phases. The slowing down of the dynamics manifests itself through a weak long time tail which extends to longer times when ϕ_f is increased and turns above ϕ_f^c into a finite asymptote which grows as shown in Fig. 5(b).

There are nevertheless strong similarities between the two dynamics, provided one concentrates on the time domain where $\phi_q(t) \simeq f_q^c$ [i.e., where $\phi_q(t)$ is small for a type A transition]. For type B dynamics, this corresponds to the so-called fast β relaxation regime and we first specialize the discussion to this case. Then, close enough to the transition, a reduction theorem holds, according to which the wave vector and time dependencies of $\phi_q(t)$ factorize, yielding

$$\phi_q(t) = f_q^c + h_q G(t). \qquad (27)$$

At the critical point, the critical decay law

$$G(t) = (t_0/t)^a \qquad (28)$$

is obtained, where a is given by Eq. (26) and t_0 is a time scale obtained by matching the short and long time dynamics. For finite values of $\phi_f - \phi_f^c$, one finds the scaling laws

$$G(t) = c_\beta g_\pm(t/\tau_\beta), \qquad \phi_f - \phi_f^c \gtrless 0, \qquad (29)$$

where the master functions $g_\pm(\hat{t})$ are the solutions of

$$\pm 1 + \lambda g_\pm(\hat{t})^2 - \frac{d}{d\hat{t}} \int_0^{\hat{t}} d\hat{\tau}\, g_\pm(\hat{t} - \hat{\tau}) g_\pm(\hat{\tau}) = 0, \qquad (30)$$

and the scaling variables obey

$$c_\beta \propto |\phi_f - \phi_f^c|^{1/2}, \qquad \tau_\beta/t_0 \propto |\phi_f - \phi_f^c|^{-1/2a}. \qquad (31)$$

For small $\hat{t}$, we have

$$g_\pm(\hat{t}) = 1/\hat{t}^a. \qquad (32)$$

For large $\hat{t}$, in the nonergodic phase, $g_+(\hat{t})$ goes to a constant and Eq. (20) results from the expression of c_β. In the same time regime, in the ergodic phase, another power law behavior sets in for $g_-(\hat{t})$, yielding the so-called von Schweidler decay law,

$$g_-(\hat{t}) = -B\hat{t}^b, \qquad (33)$$

where b is given by Eq. (26) and B is a positive constant which can be determined by matching Eq. (33) with Eq. (32) for $\hat{t} \simeq 1$. By combining the power law behaviors of c_β and τ_β in the resulting expression of $G(t)$, one recovers the divergence of τ_α, Eq. (24).

Moving now to the type A transitions, one finds that, both in the ergodic and nonergodic states, $\phi_q(t)$ essentially behaves near zero as it does when it approaches f_q^c in the glassy phase in a type B scenario. In particular, the critical decay law (28) remains valid at the transition. For finite values of $\phi_f - \phi_f^c$ and independently of its sign, Eq. (27) has to be modified in order to properly define $G(t)$ (see Ref. [18] for details), then one finds that a scaling law holds, of the form

$$G(t) = c g_+(t/\tau), \qquad (34)$$

where $g_+(\hat{t})$ is the same function as above. However, as in Eq. (21), the exponents characterizing the scaling variables c and τ are twice those for a type B transition, i.e.,

$$c \propto |\phi_f - \phi_f^c|, \qquad \tau/t_0 \propto |\phi_f - \phi_f^c|^{-1/a}. \qquad (35)$$

These behaviors are illustrated in Fig. 8, where the time evolution of $|\phi_q(t) - f_q^c|$ [simply $\phi_q(t)$ for the type A transition] at $q \simeq 7.09/d$ is plotted in a log-log scale in order to evidence the power laws (32) and (33). In this graphs, an interesting consequence of the scaling laws for small $\hat{t}$ is clearly visible, which is the symmetric departure from the

critical decay law (28) at long times for points located in the liquid and glassy phases at the same distance from the transition. This is a particularly important feature of the dynamics in the type A scenario.

The above results do not apply in the vicinity of higher-order singularities or crossing points, where a refined mathematical analysis is required [18,56,60]. A detailed discussion is beyond the scope of the present overview of the theory and we shall only mention that such liquid-glass transition points signal themselves in the dynamics through the appearance of logarithmic decay laws [18,21,56,60].

Finally, already for bulk systems, it is often quite difficult to unambiguously demonstrate that the above features are actually present in some experimental or simulation data, since, as mentioned in the introduction, the MCT offers an idealized picture of the glass transition phenomenon and there are always significant alterations to the theoretical scenario. An additional difficulty can be anticipated in the case of QA systems. Indeed, one usually has access to the total density correlation function $\phi_q^T(t)$ and not to the connected function $\phi_q(t)$. Both are related through

$$\phi_q^T(t) = \frac{S_q^c}{S_q^{ff}}\phi_q(t) + \frac{S_q^b}{S_q^{ff}}. \tag{36}$$

Thus the glassy dynamics is modulated by static factors and in particular develops itself on top of a state dependent static background. The separation in the long time behavior of $\phi_q^T(t)$ of the evolutions which are of purely static origin from those which characterize the glassy dynamics might then be delicate. This could be especially critical for type A transitions, where the signatures of the continuous transition have to be identified just on top of the slowly drifting static contribution. Figures demonstrating the problem can be found in Ref. [38].

VI. DISCUSSION AND CONCLUSION

In this paper, a mode-coupling theory for the slow dynamics of fluids adsorbed in disordered porous solids made of spherical particles frozen in random positions has been developed. Derived by properly taking into account the peculiar structure of the correlations in these systems and by including a contribution which had been forgotten in a previous work [37], its equations are found to display many appealing features. For instance, they show universality, in the sense that they do not contain any explicit reference to the precise nature of the random environment in which the fluid evolves. Also, they compare favorably with previous mode-coupling equations derived in other contexts, for the residual dynamics in the glassy phase of a bulk fluid (Sec. III) or for the equilibrium dynamics of a mean-field spin glass in a random magnetic field (Appendix C). Thus, from a formal point of view, the theory appears rather satisfactory.

Nevertheless, a few difficulties remain. First, there is the fact that, in the limit of vanishing fluid-fluid interactions, the present theory does not coincide with the MCT which can be derived by assuming from the start that there are no such interactions. Second, there is the divergence of the memory kernel for small wave vectors and the resulting spurious long time anomalies [33,62,63]. We do not believe that these issues are really harmful, even if their handling requires *ad hoc* approximations, but they are worth stressing, since their solutions would probably teach us something on the nature of the approximations underlying the MCT scheme and on possible extensions of the theory. For instance, it has been argued by Leutheusser that the inclusion of vertex corrections within a kinetic theory approach would solve the second problem, but no operational scheme was proposed for this calculation [62].

The numerical solution of the MCT equations for two simple fluid-matrix models leads to a variety of transition scenarios, which are either discontinuous for dilute matrices or continuous for dense matrices. Depending on the model, in the intermediate region where the nature of the transition changes, degenerate or genuine higher-order singularities and glass-glass transition lines are found.

Another remarkable prediction of the theory is the possibility of a reentry phenomenon for high matrix densities above the localization threshold, which has been interpreted as the signature of a decorrelation process induced by fluid-fluid collisions.

Before going further, one should note that, strictly speaking, this prediction of the theory cannot be correct in the case of hard core fluid-matrix interactions. Indeed, as recently confirmed by extensive computer simulations of the Lorentz gas [65], the localization transition is driven by the percolation transition of the matrix void space, i.e., localization occurs because, above a certain critical matrix density ϕ_m^*, the void space only consists of finite disconnected domains. In such a scenario, it is obvious that, whatever the fluid density, it is impossible to have an ergodic system above ϕ_m^*, since fluid-fluid interactions will never change the geometry of the matrix. This contradiction between the percolation theory and the MCT clearly raises the issue of the relation between the two approaches, for which we propose the following simple argument. The MCT applied to the problem of the diffusion-localization transition attempts to capture the onset of percolation in an indirect way, by giving an account of the increasingly correlated nature of the fluid-matrix collision events as the threshold is approached. In this respect, one should note that none of the static structure functions on which it is based does show a sensitivity to the phenomenon of percolation. Following Leutheusser, the theory works at the level of a self-consistent treatment of ring collision processes [62]. This turns out to be enough to predict a diffusion-localization transition, but, clearly, the infinite sequences of correlated collisions which would really reflect the permanent trapping of the fluid particle in a finite domain above the percolation threshold are missing. From this incomplete characterization of the dynamical processes escorting the percolation phenomenon, it results that the MCT diffusion-localization transition is actually an ideal version of the true percolation transition, in the usual sense that the MCT predicts ideal glass transitions, and that the theory is not able to detect that, in an exact treatement, the percolation threshold fixes an absolute limit to diffusive behavior. When fluid-fluid collisions come into play at finite fluid densities, this leaves room for the prediction of a reentry phenomenon

in contradiction with percolation theory. We believe that it is for the same reason that the MCT also misses the fact that, at any matrix density, there is always a nonvanishing probability that particles will be trapped in a finite domain disconnected from the rest of the void space, so that the exploration of the available void space is never completely ergodic [66].

It is thus clear that the prediction of a reentrant behavior of the ergodicity breaking transition line in the low fluid density domain should not be taken too literally. In fact, a reasonable expectation based on this finding is that, below the localization threshold, but in the regime where transient trapping effects are important, there might be an acceleration of the dynamics due to fluid-fluid collisions. Interestingly, such a behavior has already been observed in a computer simulation study of a two-dimensional lattice gas model with fixed randomly placed scatterers [67]. Indeed, it was found that, starting from the zero fluid density limit, the diffusion coefficient of a tagged particle first increases with the fluid density. An interpretation in terms of a decorrelation process similar to the one discussed in Sec. IV was then proposed and validated by varying the parameters of the model.

As a possible source of the difficulties of the theory, one might blame the fact that it works at the level of disorder averaged quantities. Indeed, the procedure of averaging over disorder is equivalent to an averaging over the volume of a macroscopic system, an operation in which many microscopic details of the statics and dynamics become blurred. This might confer a mean-field character to the theory, where the contribution of the matrix would actually be taken into account at the level of a diffuse effective localizing potential, with a possible loss of important local constraints. Unfortunately, this is a necessary step in order to develop a theory which is comparable in complexity with the one for bulk systems, since it allows one to consider the system as homogeneous. Some progress has recently been made on the application of the MCT to inhomogeneous situations [68], so it should be possible to relax the condition of homogeneity in order to study the dynamics of fluids confined in pores of simple geometry which are often preferred in simulation works, but there is no doubt that the more complex wave vector dependence of the resulting theory will make it harder to obtain numerical solutions of the equations.

Moreover, beyond this purely technical aspect, the present formulation in terms of disorder averaged quantities has a practical interest as well. Indeed, many real porous media are disordered and most experimental techniques measure quantities which are averaged over the volume of a macroscopic sample and thus equivalent to the disorder averages considered by the MCT. So, the current theoretical setup seems well suited for direct comparisons with experimental results. For molecular dynamics simulations, however, since rather small systems are usually considered, it might be necessary to explicitly perform the disorder average over a representative sample of matrix configurations before a comparison with the theory can be done.

Altogether, in spite of the above merely technical issues, we believe that the present mode-coupling theory represents a valuable step towards a better understanding of the slow dynamics of confined glass-forming liquids. Indeed, it remains rather simple and, since it is a microscopic approach,

it allows one to study in detail the effect on the dynamics of changes in the different ingredients of a fluid-matrix model (fluid-fluid and fluid-matrix interactions, structure of the matrix). Thus this provides us with a tool to efficiently and thoroughly explore the phenomenology of dynamics in confinement. This is clearly illustrated by our findings for two very simple systems with pure hard core interactions, which already display new and nontrivial glass transition scenarios. Then remains the question of the validation of the theoretical predictions. Because the model of the QA mixture is quite simple and the theory makes detailed predictions, molecular dynamics studies should be able to give clear-cut answers. The presently available results look rather encouraging, but more simulation work is definitely needed.

APPENDIX A: REPLICA ORNSTEIN-ZERNIKE EQUATIONS

For reference, we quote the replica OZ equations relating the various pair correlation functions in QA binary mixtures [12–15]. They read, in Fourier space,

$$\hat{h}_q^{mm} = \hat{c}_q^{mm} + n_m \hat{c}_q^{mm} \hat{h}_q^{mm}, \tag{A1a}$$

$$\hat{h}_q^{fm} = \hat{c}_q^{fm} + n_m \hat{c}_q^{fm} \hat{h}_q^{mm} + n_f \hat{c}_q^{c} \hat{h}_q^{fm}, \tag{A1b}$$

$$\hat{h}_q^{ff} = \hat{c}_q^{ff} + n_m \hat{c}_q^{fm} \hat{h}_q^{fm} + n_f \hat{c}_q^{ff} \hat{h}_q^{ff} - n_f \hat{c}_q^{b} \hat{h}_q^{b}, \tag{A1c}$$

$$\hat{h}_q^{c} = \hat{c}_q^{c} + n_f \hat{c}_q^{c} \hat{h}_q^{c}, \tag{A1d}$$

with $\hat{c}_q^{ff} = \hat{c}_q^{c} + \hat{c}_q^{b}$ and $\hat{h}_q^{ff} = \hat{h}_q^{c} + \hat{h}_q^{b}$. As usual, h and c denote total and direct correlation functions, respectively. $\hat{f}$ denotes the Fourier transform of f and the superscripts have the same meaning as for the structure factors (see Sec. II).

Using the relations

$$S_q^{mm} = 1 + n_m \hat{h}_q^{mm}, \tag{A2a}$$

$$S_q^{fm} = \sqrt{n_f n_m} \hat{h}_q^{fm}, \tag{A2b}$$

$$S_q^{c} = 1 + n_f \hat{h}_q^{c}, \tag{A2c}$$

$$S_q^{b} = n_f \hat{h}_q^{b} \tag{A2d}$$

(remember that $S_q^{ff} = S_q^{c} + S_q^{b}$, hence $S_q^{ff} = 1 + n_f \hat{h}_q^{ff}$) the OZ equations can be formally solved for the structure factors, leading to

$$S_q^{mm} = \frac{1}{1 - n_m \hat{c}_q^{mm}}, \tag{A3a}$$

$$S_q^{fm} = \frac{\sqrt{n_f n_m} \hat{c}_q^{fm}}{(1 - n_m \hat{c}_q^{mm})(1 - n_f \hat{c}_q^{c})}, \tag{A3b}$$

$$S_q^c = \frac{1}{1 - n_f \hat{c}_q^c}, \tag{A3c}$$

$$S_q^b = n_f \left[\hat{c}_q^b + n_m \frac{(\hat{c}_q^{fm})^2}{1 - n_m \hat{c}_q^{mm}} \right] \frac{1}{(1 - n_f \hat{c}_q^c)^2}. \tag{A3d}$$

APPENDIX B: DERIVATION OF THE MODE-COUPLING MEMORY KERNEL

In this appendix, the derivation of the mode-coupling part of the memory kernel is outlined. This calculation is a direct extension of the one for bulk systems which is described in its most minute details in Ref. [18].

The memory function in Eq. (11) is defined as

$$\Omega_q^2 m_q(t) = \frac{\langle R_{\mathbf{q}}(t) R_{-\mathbf{q}} \rangle}{N_f m k_B T}, \tag{B1}$$

where $R_{\mathbf{q}}(t) = \exp[i\mathcal{Q}_1 \mathcal{L} \mathcal{Q}_1 t] i\mathcal{Q}_1 \mathcal{L} g_{\mathbf{q}}^f$ is the projected random force obtained from the longitudinal momentum density fluctuation $g_{\mathbf{q}}^f(t)$ [59]. $\mathcal{L}$ is the Liouville operator of the system and $\mathcal{Q}_1$ is the complementary operator of the projector $\mathcal{P}_1$ which projects any dynamical variable onto the subspace spanned by $\delta \rho_{\mathbf{q}}^f$ and $g_{\mathbf{q}}^f$.

The calculation of the mode-coupling part of the kernel amounts to replacing $R_{\mathbf{q}}$ in Eq. (B1) by its projection $\mathcal{P}_2 R_{\mathbf{q}}$ onto the subspace spanned by $B_{\mathbf{q},\mathbf{k}} = \delta \rho_{\mathbf{k}}^f \delta \rho_{\mathbf{q}-\mathbf{k}}^f$, $C_{\mathbf{q},\mathbf{k}}^{(1)} = \delta \rho_{\mathbf{k}}^f \rho_{\mathbf{q}-\mathbf{k}}^m$, and $C_{\mathbf{q},\mathbf{k}}^{(2)} = \delta \rho_{\mathbf{k}}^f \langle \rho_{\mathbf{q}-\mathbf{k}}^f \rangle$, where we introduce the projection operator $\mathcal{P}_2$ such that

$$\mathcal{P}_2 R_{\mathbf{q}} = \sum_{\mathbf{k}}{}' \overline{\langle R_{\mathbf{q}} B_{-\mathbf{q},-\mathbf{k}} \rangle} G_{\mathbf{q},\mathbf{k}} B_{\mathbf{q},\mathbf{k}} + \sum_{\mathbf{k}} \sum_{l,l'} \overline{\langle R_{\mathbf{q}} C_{-\mathbf{q},-\mathbf{k}}^{(l)} \rangle} H_{\mathbf{q},\mathbf{k}}^{(ll')} C_{\mathbf{q},\mathbf{k}}^{(l')}. \tag{B2}$$

In this expression, we have anticipated that, within the mode-coupling approximation, $\mathcal{P}_2$ is diagonal in $\mathbf{k}$ and the subspaces spanned by the Bs and Cs are orthogonal. The prime in the first sum indicates that, to avoid double counting, the wave vectors are assumed to be ordered somehow and the sum is restricted to $\mathbf{k} < \mathbf{q} - \mathbf{k}$. $G_{\mathbf{q},\mathbf{k}}$ and $H_{\mathbf{q},\mathbf{k}}^{(ll')}$ are normalization matrices insuring that $\mathcal{P}_2 B_{\mathbf{q},\mathbf{k}} = B_{\mathbf{q},\mathbf{k}}$ and $\mathcal{P}_2 C_{\mathbf{q},\mathbf{k}}^{(l)} = C_{\mathbf{q},\mathbf{k}}^{(l)}$.

In the course of this calculation, four-point density correlation functions are generated. Thus, in order to eventually obtain closed dynamical equations, a factorization approximation is needed to express them as products of two-point density correlation functions. We follow the usual mode-coupling prescription and find that, within this approximation, the only nonvanishing four-point functions are given by

$$\overline{\langle e^{i\mathcal{Q}_1 \mathcal{L} \mathcal{Q}_1 t} B_{\mathbf{q},\mathbf{k}} B_{-\mathbf{q},-\mathbf{k}} \rangle} \simeq N_f^2 S_k^c S_{|\mathbf{q}-\mathbf{k}|}^c \phi_k(t) \phi_{|\mathbf{q}-\mathbf{k}|}(t), \tag{B3a}$$

$$\overline{\langle e^{i\mathcal{Q}_1 \mathcal{L} \mathcal{Q}_1 t} C_{\mathbf{q},\mathbf{k}}^{(1)} C_{-\mathbf{q},-\mathbf{k}}^{(1)} \rangle} \simeq N_f N_m S_k^c S_{|\mathbf{q}-\mathbf{k}|}^{mm} \phi_k(t), \tag{B3b}$$

$$\overline{\langle e^{i\mathcal{Q}_1 \mathcal{L} \mathcal{Q}_1 t} C_{\mathbf{q},\mathbf{k}}^{(2)} C_{-\mathbf{q},-\mathbf{k}}^{(2)} \rangle} \simeq N_f^2 S_k^c S_{|\mathbf{q}-\mathbf{k}|}^b \phi_k(t), \tag{B3c}$$

$$\overline{\langle e^{i\mathcal{Q}_1 \mathcal{L} \mathcal{Q}_1 t} C_{\mathbf{q},\mathbf{k}}^{(1)} C_{-\mathbf{q},-\mathbf{k}}^{(2)} \rangle} \simeq N_f \sqrt{N_f N_m} S_k^c S_{|\mathbf{q}-\mathbf{k}|}^{fm} \phi_k(t). \tag{B3d}$$

Specializing to $t=0$ and computing $\mathcal{P}_2 B_{\mathbf{q},\mathbf{k}}$ and $\mathcal{P}_2 C_{\mathbf{q},\mathbf{k}}^{(l)}$, it results that

$$G_{\mathbf{q},\mathbf{k}} = [N_f^2 S_k^c S_{|\mathbf{q}-\mathbf{k}|}^c]^{-1}, \tag{B4a}$$

$$H_{\mathbf{q},\mathbf{k}}^{(11)} = [N_f N_m S_k^c]^{-1} \frac{S_{|\mathbf{q}-\mathbf{k}|}^b}{S_{|\mathbf{q}-\mathbf{k}|}^{mm} S_{|\mathbf{q}-\mathbf{k}|}^b - (S_{|\mathbf{q}-\mathbf{k}|}^{fm})^2}, \tag{B4b}$$

$$H_{\mathbf{q},\mathbf{k}}^{(22)} = [N_f^2 S_k^c]^{-1} \frac{S_{|\mathbf{q}-\mathbf{k}|}^{mm}}{S_{|\mathbf{q}-\mathbf{k}|}^{mm} S_{|\mathbf{q}-\mathbf{k}|}^b - (S_{|\mathbf{q}-\mathbf{k}|}^{fm})^2}, \tag{B4c}$$

$$H_{\mathbf{q},\mathbf{k}}^{(12)} = -[N_f \sqrt{N_f N_m} S_k^c]^{-1} \frac{S_{|\mathbf{q}-\mathbf{k}|}^{fm}}{S_{|\mathbf{q}-\mathbf{k}|}^{mm} S_{|\mathbf{q}-\mathbf{k}|}^b - (S_{|\mathbf{q}-\mathbf{k}|}^{fm})^2}. \tag{B4d}$$

It remains to express $\overline{\langle R_{\mathbf{q}} B_{-\mathbf{q},-\mathbf{k}} \rangle} = \overline{\langle i\mathcal{Q}_1 \mathcal{L} g_{\mathbf{q}}^f B_{-\mathbf{q},-\mathbf{k}} \rangle}$ and $\overline{\langle R_{\mathbf{q}} C_{-\mathbf{q},-\mathbf{k}}^{(l)} \rangle} = \overline{\langle i\mathcal{Q}_1 \mathcal{L} g_{\mathbf{q}}^f C_{-\mathbf{q},-\mathbf{k}}^{(l)} \rangle}$. First, using Yvon's theorem, one finds

$$\overline{\langle i\mathcal{L} g_{\mathbf{q}}^f B_{-\mathbf{q},-\mathbf{k}} \rangle} = iq k_B T N_f \left[\frac{\mathbf{q} \cdot \mathbf{k}}{q^2} S_{|\mathbf{q}-\mathbf{k}|}^c + \frac{\mathbf{q} \cdot (\mathbf{q}-\mathbf{k})}{q^2} S_k^c \right], \tag{B5a}$$

$$\overline{\langle i\mathcal{L} g_{\mathbf{q}}^f C_{-\mathbf{q},-\mathbf{k}}^{(1)} \rangle} = iq k_B T \sqrt{N_f N_m} \frac{\mathbf{q} \cdot \mathbf{k}}{q^2} S_{|\mathbf{q}-\mathbf{k}|}^{fm}, \tag{B5b}$$

$$\overline{\langle i\mathcal{L} g_{\mathbf{q}}^f C_{-\mathbf{q},-\mathbf{k}}^{(2)} \rangle} = iq k_B T N_f \frac{\mathbf{q} \cdot \mathbf{k}}{q^2} S_{|\mathbf{q}-\mathbf{k}|}^b. \tag{B5c}$$

Then, with the help of the extension of the convolution approximation [69] to QA systems,

$$\overline{\langle \delta \rho_{\mathbf{q}}^f \delta \rho_{-\mathbf{k}}^f \delta \rho_{-\mathbf{q}+\mathbf{k}}^f \rangle} = N_f S_q^c S_k^c S_{|\mathbf{q}-\mathbf{k}|}^c, \tag{B6a}$$

$$\overline{\langle \delta \rho_{\mathbf{q}}^f \delta \rho_{-\mathbf{k}}^f \rho_{-\mathbf{q}+\mathbf{k}}^m \rangle} = \sqrt{N_f N_m} S_q^c S_k^c S_{|\mathbf{q}-\mathbf{k}|}^{fm}, \tag{B6b}$$

$$\overline{\langle \delta \rho_{\mathbf{q}}^f \delta \rho_{-\mathbf{k}}^f \langle \rho_{-\mathbf{q}+\mathbf{k}}^f \rangle \rangle} = N_f S_q^c S_k^c S_{|\mathbf{q}-\mathbf{k}|}^b, \tag{B6c}$$

it follows that

$$\overline{\langle i\mathcal{P}_1 \mathcal{L} g_{\mathbf{q}}^f B_{-\mathbf{q},-\mathbf{k}} \rangle} = iq k_B T N_f S_k^c S_{|\mathbf{q}-\mathbf{k}|}^c, \tag{B7a}$$

$$\overline{\langle i\mathcal{P}_1 \mathcal{L} g_{\mathbf{q}}^f C_{-\mathbf{q},-\mathbf{k}}^{(1)} \rangle} = iq k_B T \sqrt{N_f N_m} S_k^c S_{|\mathbf{q}-\mathbf{k}|}^{fm}, \tag{B7b}$$

$$\overline{\langle i\mathcal{P}_1 \mathcal{L} g_{\mathbf{q}}^f C_{-\mathbf{q},-\mathbf{k}}^{(2)} \rangle} = iq k_B T N_f S_k^c S_{|\mathbf{q}-\mathbf{k}|}^b. \tag{B7c}$$

The desired results are obtained by substracting the matching equations.

We might now complete the explicit calculation of $\mathcal{P}_2 R_{\mathbf{q}}$. Indeed, if we define

$$v_{\mathbf{q},\mathbf{k}} = \overline{\langle R_{\mathbf{q}} B_{-\mathbf{q},-\mathbf{k}} \rangle} G_{\mathbf{q},\mathbf{k}}, \tag{B8}$$

$$w_{\mathbf{q},\mathbf{k}}^{(1)} = \overline{\langle R_{\mathbf{q}} C_{-\mathbf{q},-\mathbf{k}}^{(1)} \rangle} H_{\mathbf{q},\mathbf{k}}^{(11)} + \overline{\langle R_{\mathbf{q}} C_{-\mathbf{q},-\mathbf{k}}^{(2)} \rangle} H_{\mathbf{q},\mathbf{k}}^{(21)}, \tag{B9}$$

$$w_{\mathbf{q},\mathbf{k}}^{(2)} = \overline{\langle R_{\mathbf{q}} C_{-\mathbf{q},-\mathbf{k}}^{(1)} \rangle} H_{\mathbf{q},\mathbf{k}}^{(12)} + \overline{\langle R_{\mathbf{q}} C_{-\mathbf{q},-\mathbf{k}}^{(2)} \rangle} H_{\mathbf{q},\mathbf{k}}^{(22)}, \tag{B10}$$

such that

$$\mathcal{P}_2 R_{\mathbf{q}} = \sum_{\mathbf{k}}{}' v_{\mathbf{q},\mathbf{k}} B_{\mathbf{q},\mathbf{k}} + \sum_{\mathbf{k}} w_{\mathbf{q},\mathbf{k}}^{(1)} C_{\mathbf{q},\mathbf{k}}^{(1)} + w_{\mathbf{q},\mathbf{k}}^{(2)} C_{\mathbf{q},\mathbf{k}}^{(2)}, \quad \text{(B11)}$$

the above results immediately lead to

$$v_{\mathbf{q},\mathbf{k}} = \frac{iq k_B T}{N_f} \left[\frac{\mathbf{q} \cdot \mathbf{k}}{q^2} \frac{1}{S_k^c} + \frac{\mathbf{q} \cdot (\mathbf{q} - \mathbf{k})}{q^2} \frac{1}{S_{|\mathbf{q}-\mathbf{k}|}^c} - 1 \right], \quad \text{(B12)}$$

$$w_{\mathbf{q},\mathbf{k}}^{(1)} = 0, \quad \text{(B13)}$$

$$w_{\mathbf{q},\mathbf{k}}^{(2)} = \frac{iq k_B T}{N_f} \left[\frac{\mathbf{q} \cdot \mathbf{k}}{q^2} \frac{1}{S_k^c} - 1 \right]. \quad \text{(B14)}$$

Note the vanishing of the fluid-matrix contribution.

Eventually, injecting the resulting expression of $\mathcal{P}_2 R_{\mathbf{q}}$ into

$$\Omega_q^2 m_q^{\text{(MC)}}(t) = \frac{\overline{\langle \mathcal{P}_2 R_{\mathbf{q}}(t) \mathcal{P}_2 R_{-\mathbf{q}} \rangle}}{N_f m k_B T}, \quad \text{(B15)}$$

one obtains Eqs. (13) and (14) after a few elementary steps.

Exactly the same calculation can be done with subsets of the above three quadratic variables. One then easily demonstrates that, if only $\delta\rho_{\mathbf{k}}^f \delta\rho_{\mathbf{q}-\mathbf{k}}^f$ and $\delta\rho_{\mathbf{k}}^f \langle \rho_{\mathbf{q}-\mathbf{k}}^f \rangle$ are considered, the same equations are obtained, while, if one works with $\delta\rho_{\mathbf{k}}^f \delta\rho_{\mathbf{q}-\mathbf{k}}^f$ and $\delta\rho_{\mathbf{k}}^f \rho_{\mathbf{q}-\mathbf{k}}^m$, the equations of Ref. [37] are reproduced, which reduce to those of Refs. [29–31] in the zero fluid density limit.

APPENDIX C: MEAN-FIELD SPIN GLASS IN A RANDOM MAGNETIC FIELD

A fruitful source of new theoretical developments on the physics of glassy systems has been the finding that the MCT provides an exact description of the equilibrium dynamics of a certain class of mean-field spin-glass models with multi-spin interactions [70–72]. In this appendix, based on Ref. [73] (the interested reader is referred to this paper for details), we show that the equations describing the dynamics of such a mean-field spin-glass model in a random magnetic field reproduce the structure of those of the MCT for a fluid in a random environment. Thus, the correspondence between the two approaches still holds in the presence of an external source of disorder.

We consider the fully connected mean-field spherical spin-glass model with three spin interactions in a random magnetic field, whose Hamiltonian is

$$H_J[\mathbf{s}] = - \sum_{1 \le i < j < k \le N} J_{ijk}^{(3)} s_i s_j s_k - \sum_{1 \le i \le N} J_i^{(1)} s_i, \quad \text{(C1)}$$

where the spins s_i are N real variables subject to the constraint $\sum_{i=1}^N s_i^2 = N$, and the random coupling constants $J_{ijk}^{(3)}$ and fields $J_i^{(1)}$ are uncorrelated zero mean Gaussian variables with variances $3J_3^2/N^2$ and $J_1^2/2$, respectively. In zero field ($J_1 = 0$), this model is known to generate the quadratic memory kernel introduced in Refs. [16] and [17] as a one wave-vector approximation to the bulk MCT functional. Thus it is especially suitable for our purpose, since it displays nonlinearities of the same degree as in the MCT.

In the presence of a random magnetic field, just like QA mixtures are characterized by static frozen density fluctua-

tions, the present spin-glass model is characterized by static frozen local magnetizations $\langle s_i \rangle$ which vanish when the average over disorder (both on couplings and fields) is performed. Accordingly, we might define $\delta s_i(t) = s_i(t) - \langle s_i \rangle$ and introduce three correlation functions, which are the analogues of S_q^b, S_q^c, and $\phi_q(t)$. They are, respectively, the two overlap functions

$$q_b = \frac{1}{N} \sum_{i=1}^N \overline{\langle s_i \rangle^2} \quad \text{(C2)}$$

and

$$q_c = \frac{1}{N} \sum_{i=1}^N \overline{\langle (\delta s_i)^2 \rangle}, \quad \text{(C3)}$$

which obey $q_b + q_c = 1$, and the normalized connected spin correlation function,

$$\phi(t) = \frac{1}{N q_c} \sum_{i=1}^N \overline{\langle \delta s_i(t) \delta s_i(0) \rangle}. \quad \text{(C4)}$$

The exact solution of the Langevin dynamics of the model using standard methods [73] provides us with an equation for the time evolution of $\phi(t)$ which reads, for a high enough temperature T,

$$\dot{\phi}(t) + \frac{1}{q_c} \phi(t) + \frac{1}{q_c} \int_0^t d\tau \, m(t - \tau) \dot{\phi}(\tau) = 0, \quad \text{(C5a)}$$

with

$$m(t) = \frac{1}{2} q_c \left[\frac{3J_3^2}{T^2} \right] q_c^2 \phi(t)^2 + q_c \left[\frac{3J_3^2}{T^2} \right] q_c q_b \phi(t). \quad \text{(C5b)}$$

A direct comparison of these equations with those of Sec. II immediately shows that both sets of equations exactly have the same formal structure. In particular, beyond the simple fact that the memory functions are similar polynomials of the dynamical correlation functions, the same parametrization in terms of connected and disconnected static correlations is found.

We conclude with two short remarks. First, as for QA mixtures, we note that the external random field does not enter explicitly in the above equations (no J_1 is present). Because the model is exactly soluble, it is easy to understand how this happens. In fact, the details of the random field are only needed for the computation of the static correlations, through the equality

$$\frac{J_1^2}{2T^2} + \frac{3J_3^2}{2T^2} q_b^2 = \frac{q_b}{(1 - q_b)^2}. \quad \text{(C6)}$$

Once this calculation is done, they can be forgotten. The same is probably true for fluids in random environments and this supports the assumption that the MCT equations for QA systems actually have a wider domain of applicability, provided they are expressed in terms of fluid quantities only.

Second, it can be shown that Eq. (C5) also describes the residual relaxation of the present spin-glass model in zero

field, when the system is equilibrated in its low temperature phase and the total spin correlation function has a nonvanishing infinite time limit q [74]. Then, q_b and q_c simply have to be replaced by q and $1-q$. Thus, in the present model, the difference discussed in Sec. III between self-induced glassiness and the effect of a quenched random field does not seem to exist. This could have been anticipated, since by construction, fully connected models are unable to capture phenomena which only show up in the wave vector dependence of the coupling constants in fluid systems.

[1] *Proceedings of the International Workshop on Dynamics in Confinement*, edited by R. Zorn, B. Frick, and H. Büttner [J. Phys. IV **IV10**, Pr7-203 (2000)].

[2] *Proceedings of the Second International Workshop on Dynamics in Confinement*, edited by B. Frick, M. Koza, and R. Zorn [Eur. Phys. J. E **12**, 3-204 (2003)].

[3] M. Alcoutlabi and G. B. McKenna, J. Phys.: Condens. Matter **17**, R461 (2005).

[4] C. Alba-Simionesco, B. Coasne, G. Dosseh, G. Dudziak, K. E. Gubbins, R. Radhakrishnan, and M. Sliwinska-Bartkowiak, J. Phys.: Condens. Matter **18**, R15 (2006).

[5] H. Sillescu, J. Non-Cryst. Solids **243**, 81 (1999).

[6] M. D. Ediger, Annu. Rev. Phys. Chem. **51**, 99 (2000).

[7] R. Richert, J. Phys.: Condens. Matter **14**, R703 (2002).

[8] L. Berthier, G. Biroli, J.-P. Bouchaud, L. Cipelletti, D. El Masri, D. L'Hôte, F. Ladieu, and M. Pierno, Science **310**, 1797 (2005).

[9] W. G. Madden and E. D. Glandt, J. Stat. Phys. **51**, 537 (1988).

[10] W. G. Madden, J. Chem. Phys. **96**, 5422 (1992).

[11] D. M. Ford and E. D. Glandt, J. Chem. Phys. **100**, 2391 (1994).

[12] J. A. Given and G. Stell, J. Chem. Phys. **97**, 4573 (1992).

[13] E. Lomba, J. A. Given, G. Stell, J. J. Weis, and D. Levesque, Phys. Rev. E **48**, 233 (1993).

[14] J. A. Given and G. Stell, Physica A **209**, 495 (1994).

[15] M.-L. Rosinberg, G. Tarjus, and G. Stell, J. Chem. Phys. **100**, 5172 (1994).

[16] U. Bengtzelius, W. Götze, and A. Sjölander, J. Phys. C **17**, 5915 (1984).

[17] E. Leutheusser, Phys. Rev. A **29**, 2765 (1984).

[18] W. Götze, in *Liquids, Freezing and Glass Transition*, edited by J.-P. Hansen, D. Levesque, and J. Zinn-Justin (North-Holland, Amsterdam, 1991), pp. 287–503.

[19] W. Götze and L. Sjögren, Rep. Prog. Phys. **55**, 241 (1992).

[20] W. Götze, J. Phys.: Condens. Matter **11**, A1 (1999).

[21] L. Fabbian, W. Götze, F. Sciortino, P. Tartaglia, and F. Thiery, Phys. Rev. E **59**, R1347 (1999); **60**, 2430 (1999); J. Bergenholtz and M. Fuchs, *ibid.* **59**, 5706 (1999); K. Dawson, G. Foffi, M. Fuchs, W. Götze, F. Sciortino, M. Sperl, P. Tartaglia, T. Voigtmann, and E. Zaccarelli, *ibid.* **63**, 011401 (2001).

[22] S.-H. Chong and W. Götze, Phys. Rev. E **65**, 041503 (2002); **65**, 051201 (2002).

[23] P. Gallo, M. Rovere, and E. Spohr, Phys. Rev. Lett. **85**, 4317 (2000); J. Chem. Phys. **113**, 11324 (2000).

[24] P. Gallo, R. Pellarin, and M. Rovere, Europhys. Lett. **57**, 212 (2002); Phys. Rev. E **67**, 041202 (2003); **68**, 061209 (2003).

[25] P. Scheidler, W. Kob, and K. Binder, J. Phys. Chem. B **108**, 6673 (2004).

[26] K. Kim, Europhys. Lett. **61**, 790 (2003).

[27] R. Chang, K. Jagannathan, and A. Yethiraj, Phys. Rev. E **69**, 051101 (2004).

[28] J. Mittal, J. R. Errington, and T. M. Truskett, Phys. Rev. E **74**, 040102(R) (2006).

[29] W. Götze, E. Leutheusser, and S. Yip, Phys. Rev. A **23**, 2634 (1981).

[30] E. Leutheusser, Phys. Rev. A **28**, 2510 (1983).

[31] G. Szamel, Europhys. Lett. **65**, 498 (2004).

[32] W. Götze, Solid State Commun. **27**, 1393 (1978); J. Phys. C **12**, 1279 (1979).

[33] W. Götze, Philos. Mag. B **43**, 219 (1981).

[34] J. S. Thakur and D. Neilson, Phys. Rev. B **54**, 7674 (1996); **59**, R5280 (1999); J. Phys.: Condens. Matter **12**, 4483 (2000).

[35] For instance, the theory of Ref. [34] amounts to setting $\hat{c}_q^c \equiv 0$ in Eq. (14b), but not in Eq. (14a).

[36] G. Migliorini, V. G. Rostiashvili, and T. A. Vilgis, Eur. Phys. J. B **33**, 61 (2003).

[37] V. Krakoviack, Phys. Rev. Lett. **94**, 065703 (2005).

[38] V. Krakoviack, J. Phys.: Condens. Matter **17**, S3565 (2005).

[39] G. I. Menon and C. Dasgupta, Phys. Rev. Lett. **73**, 1023 (1994).

[40] E. Kierlik, M.-L. Rosinberg, and G. Tarjus, J. Stat. Phys. **94**, 805 (1999).

[41] For an ideal gas in any type of statistically homogeneous random environment, one finds that $c^c(r)=h^c(r)\equiv 0$ and that $c^b(r)$ and $h^b(r)$ are independent of n_f.

[42] Similar discrepancies appear generically when different routes are followed to derive the MCT equations for the tagged particle dynamics in a QA system. They will be discussed in more detail, with their quantitative consequences, in a forthcoming paper [V. Krakoviack (in preparation)].

[43] J.-P. Bouchaud and M. Mézard, J. Phys. I **4**, 1109 (1994).

[44] E. Marinari, G. Parisi, and F. Ritort, J. Phys. A **27**, 7615 (1994); **27**, 7647 (1994).

[45] L. F. Cugliandolo, J. Kurchan, G. Parisi, and F. Ritort, Phys. Rev. Lett. **74**, 1012 (1995).

[46] L. F. Cugliandolo, J. Kurchan, R. Monasson, and G. Parisi, J. Phys. A **29**, 1347 (1996).

[47] W. Götze and M. R. Mayr, Phys. Rev. E **61**, 587 (2000).

[48] W. Götze, in *Amorphous and Liquid Materials*, edited by M. Lüscher, G. Fritsch, and G. Jacucci, NATO Advanced Study Institute, Series E: Applied Sciences (Nijhoff, Dordrecht, 1987), Vol. 118, pp. 34–81.

[49] D. Chandler, J. Phys.: Condens. Matter **3**, F1 (1991).

[50] J. Bosse and J. S. Thakur, Phys. Rev. Lett. **59**, 998 (1987).

[51] V. Krakoviack, E. Kierlik, M.-L. Rosinberg, and G. Tarjus, J. Chem. Phys. **115**, 11289 (2001).

[52] A. Meroni, D. Levesque, and J.-J. Weis, J. Chem. Phys. **105**, 1101 (1996).

[53] T. Franosch, M. Fuchs, W. Götze, M. R. Mayr, and A. P. Singh, Phys. Rev. E **55**, 7153 (1997).

[54] The possible values of Δ are limited by the method of solution of the OZ/PY equations on a real space grid of equally spaced points with a step size commensurate to the hard core diameter d. For our calculation, the present choice of Δ offers the closest match with the value $\Delta = 0.4/d$ used in Ref. [53], where analytic expressions for the structure functions were readily available.

[55] W. Götze and L. Sjögren, J. Math. Anal. Appl. **195**, 230 (1995).

[56] M. Sperl, Phys. Rev. E **69**, 011401 (2004).

[57] R. D. Kaminsky and P. A. Monson, J. Chem. Phys. **95**, 2936 (1991).

[58] E. Kierlik, M.-L. Rosinberg, G. Tarjus, and P. A. Monson, J. Chem. Phys. **106**, 264 (1997).

[59] J.-P. Hansen and I. R. McDonald, *Theory of Simple Liquids*, 2nd ed. (Academic Press, London, 1986).

[60] W. Götze and M. Sperl, Phys. Rev. E **66**, 011405 (2002); M. Sperl, *ibid.* **68**, 031405 (2003); W. Götze and M. Sperl, J. Phys.: Condens. Matter **16**, S4807 (2004).

[61] A. J. Moreno and J. Colmenero, J. Chem. Phys. **124**, 184906 (2006); Phys. Rev. E **74**, 021409 (2006); J. Chem. Phys. **125**, 164507 (2006).

[62] E. Leutheusser, Phys. Rev. A **28**, 1762 (1983).

[63] F. Höfling, E. Frey, and T. Franosch (unpublished).

[64] M. Fuchs, W. Götze, I. Hofacker, and A. Latz, J. Phys.: Condens. Matter **3**, 5047 (1991).

[65] F. Höfling, T. Franosch, and E. Frey, Phys. Rev. Lett. **96**, 165901 (2006).

[66] J. Kertész and J. Metzger, J. Phys. A **16**, L735 (1983).

[67] C. Oleksy, J. Phys. A **24**, L751 (1991).

[68] G. Biroli, J.-P. Bouchaud, K. Miyazaki, and D. R. Reichman, Phys. Rev. Lett. **97**, 195701 (2006).

[69] H. W. Jackson and E. Feenberg, Rev. Mod. Phys. **34**, 686 (1962).

[70] T. R. Kirkpatrick and D. Thirumalai, Phys. Rev. Lett. **58**, 2091 (1987); Phys. Rev. B **36**, 5388 (1987).

[71] A. Crisanti, H. Horner, and H.-J. Sommers, Z. Phys. B: Condens. Matter **92**, 257 (1993).

[72] J.-P. Bouchaud, L. F. Cugliandolo, J. Kurchan, and M. Mézard, Physica A **226**, 243 (1996).

[73] S. Ciuchi and A. Crisanti, Europhys. Lett. **49**, 754 (2000).

[74] A. Barrat, R. Burioni, and M. Mézard, J. Phys. A **29**, L81 (1996).